Analytic electron and ion electrical-conductivity tensors of a fully ionized two-component plasma

W. A. Stygar,[1] C. M. Provencher,[1] K. Tummel,[1] and D. R. Welch[2]
[1]*Lawrence Livermore National Laboratory, Livermore, California 94550, USA*
[2]*Voss Scientific, Albuquerque, New Mexico 87108, USA*

(Received 15 December 2025; accepted 28 July 2026; published 3 November 2026)

We have developed explicit analytic expressions for the electron and ion electrical-conductivity tensors of a fully ionized two-component plasma. We assume the plasma is nondegenerate, nonrelativistic, and subject to electric and magnetic fields. The conductivity tensors give the Pedersen, Hall, and Birkeland currents of the electrons and ions as functions of the electric field, magnetic field, and plasma parameters. (By definition, the electron and ion Pedersen currents are those that flow in the direction of the component of **E** that is perpendicular to **B**. The electron and ion Hall currents flow in the $-\mathbf{E}\times\mathbf{B}$ and $\mathbf{E}\times\mathbf{B}$ directions, respectively. The electron and ion Birkeland currents flow in the direction of the component of **E** that is parallel to **B**.) We derive the conductivity tensors from Lorentz-force, kinetic, modified-two-fluid, and standard-two-fluid models of a plasma. The Lorentz-force model is based on the electron and ion Lorentz-force equations, and the probability distribution of random collisions. The kinetic model is based on the electron and ion Boltzmann equations in the relaxation-time approximation. The modified-two-fluid model is derived from the kinetic model, and differs from the well-known standard-two-fluid model. The Lorentz-force, kinetic, and modified-two-fluid models are in agreement and, in the steady state, predict the following: In the collisionless limit ($\omega_{ce}\tau\to\infty$, $\omega_{ci}\tau\to\infty$), the electron and ion Pedersen currents $\to 0$, whereas the electron and ion Hall currents dominate. In the collisional limit ($\omega_{ce}\tau\to 0$, $\omega_{ci}\tau\to 0$), the Pedersen currents dominate, whereas the Hall currents $\to 0$. (The quantities ω_{ce} and ω_{ci} are the electron- and ion-cyclotron frequencies, respectively; τ is the interparticle momentum-transfer collision time.) The results are consistent with elementary physical considerations. The standard-two-fluid model predicts instead that, in the steady state, the Pedersen currents are identically 0, and the Hall currents dominate, for all values of $\omega_{ce}\tau$ and $\omega_{ci}\tau$ (when $\mathbf{B}\neq 0$). The discrepancies with the Lorentz-force, kinetic, and modified-two-fluid models are caused by the collision terms of the standard-two-fluid model.

DOI: 10.1103/d898-7tzb

I. INTRODUCTION

We consider a nondegenerate, nonrelativistic fully ionized plasma. We assume the plasma consists of electrons and one ion species with charge state Z. We assume the plasma is quasineutral, and the electrons and ions are at the same temperature T. We assume also that the temperature, number densities, and fluid velocities of the two plasma species have negligible spatial gradients. In addition, we assume the plasma is subject to uniform electric and magnetic fields, **E** and **B**, respectively.

We model the plasma with the coordinate system illustrated by Fig. 1. Without loss of generality, we assume throughout the article that **B** is in the positive z direction; i.e., that $\mathbf{B}=B_z\,\mathbf{e}_z$. (The quantities $\mathbf{e}_x$, $\mathbf{e}_y$, and $\mathbf{e}_z$ are unit vectors in the x, y, and z directions, respectively.)

The principal objective of the article is to estimate for such a plasma the currents that flow within; i.e., the Pedersen, Hall, and Birkeland currents. By definition, the electron and ion Pedersen currents are those that flow in the direction of the component of **E** that is perpendicular to **B**. The electron and ion Hall currents flow in the $-\mathbf{E}\times\mathbf{B}$ and $\mathbf{E}\times\mathbf{B}$ directions, respectively. The electron and ion Birkeland currents flow in the direction of the component of **E** that is parallel to **B**.

One example of a plasma of interest is that which is found within a magnetically insulated transmission line (MITL) [1–22]. A MITL is a crossed-field device: It subjects the charged particles between its electrodes to perpendicular **E** and **B** fields. When operated, a MITL is under vacuum *initially*: The space between the MITL's anode and cathode electrodes typically begins at a pressure in the 10^{-4}–10^{-8} torr range. However, when operated at sufficiently high electromagnetic-power densities, particles evolve from the MITL-electrode surfaces during operation, enter the anode-cathode gap of the MITL, and become ionized. It is often desired to minimize the Pedersen and Hall currents (Fig. 1) carried by such a plasma.

The Pedersen, Hall, and Birkeland currents within a plasma subject to **E** and **B** fields can be estimated with electron and ion electrical-conductivity tensors. In this article, we derive explicit analytic expressions for the tensors from Lorentz-force, kinetic, modified-two-fluid, and standard-two-fluid models of a plasma. The models are outlined by Secs. II, III, IV, and V, respectively.

Section VI compares time-dependent electron and ion fluid velocities as predicted by the modified- and standard-two-fluid models. Section VII presents additional comments on the standard-two-fluid model. Results of the article are

Published by the American Physical Society under the terms of the Creative Commons Attribution 4.0 International license. Further distribution of this work must maintain attribution to the author(s) and the published article's title, journal citation, and DOI.

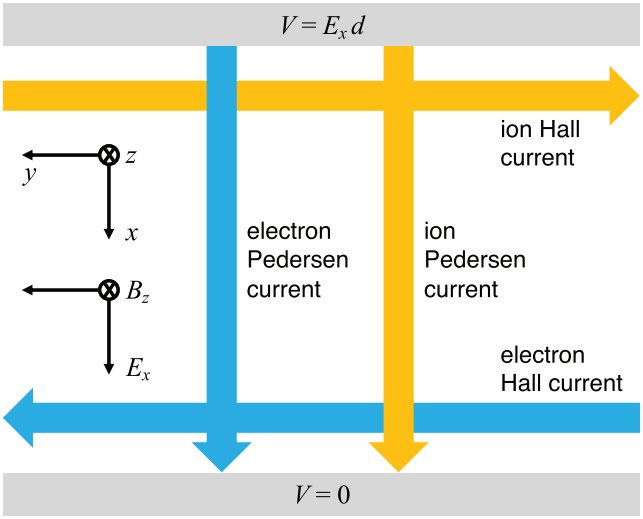


FIG. 1. Coordinate system assumed by the article. Without loss of generality, we assume throughout that $\mathbf{B} = B_z\,\mathbf{e}_z$. The figure illustrates directions of the Pedersen and Hall currents when $\mathbf{E} = E_x\,\mathbf{e}_x$. The electrical-conductivity tensors developed by the article make the more general assumption that $\mathbf{E} = E_x\,\mathbf{e}_x + E_y\,\mathbf{e}_y + E_z\,\mathbf{e}_z$. When $E_z \neq 0$, the electron and ion Birkeland currents flow in the direction of E_z. The quantity V is the potential difference across the plasma, and d is the plasma thickness.

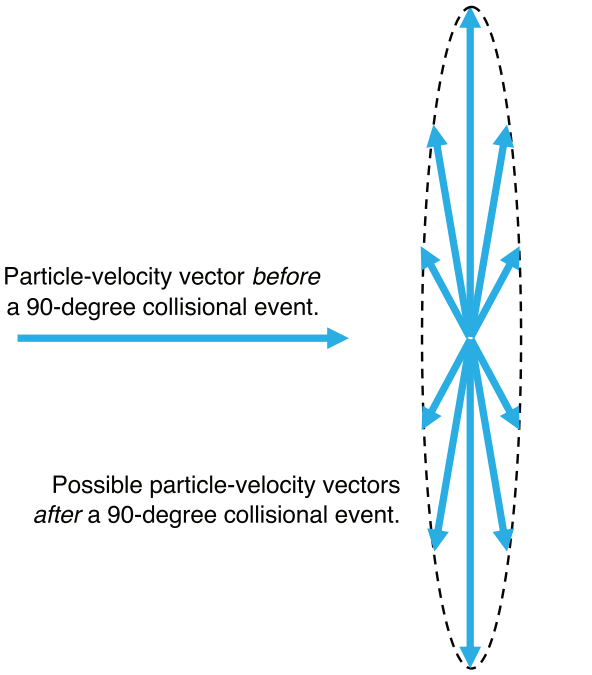


FIG. 2. We define a collision to be an event that consists of a single 90° deflection, or a number of smaller deviations that combined result in a 90° deflection. Such a collisional event, which is illustrated here, reduces the particle's initial forward-directed velocity to 0. We assume that after such a collisional event, the velocity is randomly distributed azimuthally, and hence the postcollision velocity of the particle, averaged over a large number of particles, equals 0 [23–25]. (We observe that the velocity-reset assumption is *not* explicitly made by the kinetic, modified-two-fluid, and standard-two-fluid models outlined by Secs. III–V.)

summarized by Sec. VIII. Appendices A and B outline derivations of the tensors presented by Secs. II and III, respectively.

Except for Sec. VII A, the article assumes the laboratory frame of reference: a local inertial reference frame that is centered on the laboratory and contains the plasma under consideration. This is the frame within which the laboratory is at rest, and measurements are made. The article assumes plasma conditions are such that runaway electrons and ions can be neglected. Equations in this article are in cgs-Gaussian units throughout.

II. LORENTZ-FORCE MODEL

A. Electron and ion Lorentz-force equations

The Lorentz-force model of a plasma considered by this article is based on the nonrelativistic electron and ion Lorentz-force equations:

$$\mathbf{F}_e = m_e \frac{d\mathbf{v}_e}{dt} = -e\mathbf{E} - \frac{e}{c}(\mathbf{v}_e \times \mathbf{B}), \tag{1}$$

$$\mathbf{F}_i = m_i \frac{d\mathbf{v}_i}{dt} = Ze\mathbf{E} + \frac{Ze}{c}(\mathbf{v}_i \times \mathbf{B}). \tag{2}$$

The quantity $\mathbf{F}_e$ is the force on an electron, m_e is the electron mass, $\mathbf{v}_e$ is the electron particle velocity, e is the absolute value of the elementary charge, $\mathbf{E}$ is the electric field, c is the speed of light, $\mathbf{B}$ is the magnetic field, $\mathbf{F}_i$ is the force on an ion, m_i is the ion mass, $\mathbf{v}_i$ is the ion particle velocity, and Z is the ionization charge state.

B. Electron and ion conductivity tensors

Beginning with Eqs. (1) and (2), and assuming $\mathbf{E} = E_x\,\mathbf{e}_x + E_y\,\mathbf{e}_y + E_z\,\mathbf{e}_z$ and $\mathbf{B} = B_z\,\mathbf{e}_z$, we derive in Appendix A electron and ion electrical-conductivity tensors. The derivation closely follows those given by Parks [23] and Piel [24]. These references make use of the probability distribution of random collisions as described by Feynman [25].

Appendix A makes a velocity-reset assumption identical to that of Parks [23], Piel [24], and Feynman [25]. We define a collision to be an event that consists of a single 90° deflection, or a number of smaller deviations that combined result in a 90° deflection (Fig. 2). Such a collision reduces the particle's initial forward-directed velocity to 0. We assume that, after a collision, the direction of the velocity perpendicular to that of the initial forward direction is randomly distributed. Hence as suggested by Fig. 2, the postcollision velocity is, averaged over many particles, equal to 0. (We note that the velocity-reset assumption is *not* explicitly made by the kinetic, modified-two-fluid, and standard-two-fluid models outlined by Secs. III–V.)

The electron conductivity tensor $\underline{\sigma}_e$ can be expressed as follows:

$$\mathbf{j}_e = \underline{\sigma}_e \mathbf{E}, \tag{3}$$

$$\underline{\sigma}_e = \begin{pmatrix} \dfrac{\sigma_e}{(1+\omega_{ce}^2\tau_{ei}^2)} & \dfrac{-\omega_{ce}\tau_{ei}\sigma_e}{(1+\omega_{ce}^2\tau_{ei}^2)} & 0 \\ \dfrac{\omega_{ce}\tau_{ei}\sigma_e}{(1+\omega_{ce}^2\tau_{ei}^2)} & \dfrac{\sigma_e}{(1+\omega_{ce}^2\tau_{ei}^2)} & 0 \\ 0 & 0 & \sigma_e \end{pmatrix}, \tag{4}$$

$$\sigma_e = \frac{n_e e^2 \tau_{ei}}{m_e}, \tag{5}$$

$$\omega_{ce} = \frac{eB_z}{m_e c}. \tag{6}$$

The quantity $\mathbf{j}_e$ is the electron current density, σ_e is the scalar electron conductivity, τ_{ei} is the electron-ion momentum-transfer collision time, ω_{ce} is the nonrelativistic electron cyclotron frequency, and n_e is the electron number density.

The ion conductivity tensor $\underline{\sigma}_i$ has a similar form:

$$\mathbf{j}_i = \underline{\sigma}_i \mathbf{E}, \tag{7}$$

$$\underline{\sigma}_i = \begin{pmatrix} \frac{\sigma_i}{(1+\omega_{ci}^2\tau_{ie}^2)} & \frac{\omega_{ci}\tau_{ie}\sigma_i}{(1+\omega_{ci}^2\tau_{ie}^2)} & 0 \\ \frac{-\omega_{ci}\tau_{ie}\sigma_i}{(1+\omega_{ci}^2\tau_{ie}^2)} & \frac{\sigma_i}{(1+\omega_{ci}^2\tau_{ie}^2)} & 0 \\ 0 & 0 & \sigma_i \end{pmatrix}, \tag{8}$$

$$\sigma_i = \frac{n_i Z^2 e^2 \tau_{ie}}{m_i}, \tag{9}$$

$$\omega_{ci} = \frac{ZeB_z}{m_i c}. \tag{10}$$

The quantity $\mathbf{j}_i$ is the ion current density, σ_i is the scalar ion conductivity, τ_{ie} is the ion-electron momentum-transfer collision time, ω_{ci} is the nonrelativistic ion cyclotron frequency, and n_i is the ion number density.

The total current density within the plasma is the sum of the electron and ion components:

$$\mathbf{j} = \mathbf{j}_e + \mathbf{j}_i = (\underline{\sigma}_e \mathbf{E}) + (\underline{\sigma}_i \mathbf{E}). \tag{11}$$

C. Interparticle momentum-transfer collision time

Throughout this article we make the simplifying assumption that τ_{ei} and τ_{ie} can be approximated as constants. We determine the relationship between τ_{ei} and τ_{ie} by considering the electron and ion Birkeland currents, j_{ez} and j_{iz}, respectively. As suggested by Eqs. (3), (4), (7), and (8), these can be expressed as follows:

$$j_{ez} = -n_e e u_{ez} = \sigma_e E_z, \tag{12}$$

$$j_{iz} = n_i Z e u_{iz} = \sigma_i E_z. \tag{13}$$

The quantities u_{ez} and u_{iz} are z components of the electron and ion fluid velocities.

Throughout the article we assume quasineutrality:

$$n_e = Z n_i. \tag{14}$$

The magnetic field $\mathbf{B}$ does not affect the electron and ion Birkeland currents. Hence since the plasma is quasineutral, the total kinetic momentum of the electrons and ions in the z direction must be conserved:

$$n_e m_e u_{ez} + n_i m_i u_{iz} = 0. \tag{15}$$

Combining Eqs. (5), (9), and (12)–(15) we find that

$$\tau_{ei} = \tau_{ie} = \tau. \tag{16}$$

We define τ to be the interparticle momentum-transfer collision time.

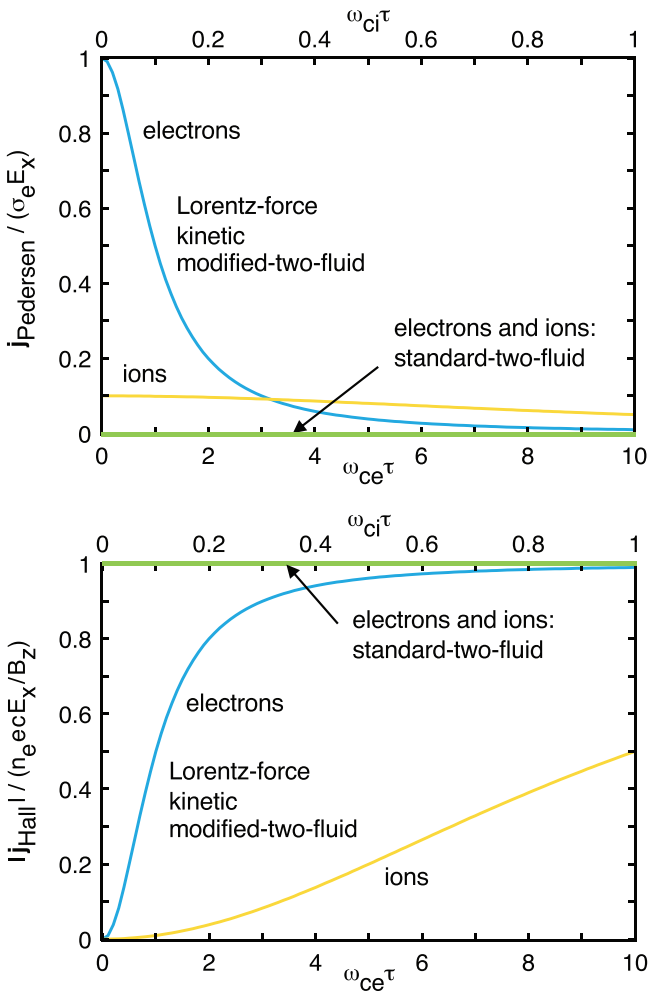


FIG. 3. Steady-state Pedersen and Hall currents as predicted by the Lorentz-force, kinetic, modified-two-fluid, and standard-two-fluid models of a plasma. The currents are plotted as functions of $\omega_{ce}\tau$ and $\omega_{ci}\tau$. To facilitate comparison of the currents we set $m_i = 10m_e$. The plots make the simplifying assumptions that $Z = 1$ and $\mathbf{E} = E_x\,\mathbf{e}_x$. In the steady state, the standard-two-fluid model is consistent with the Lorentz-force, kinetic, and modified-two-fluid models in the collisionless limit ($\omega_{ce}\tau \to \infty$, $\omega_{ci}\tau \to \infty$). The four models are also consistent when $\mathbf{B} = 0$ (Sec. V C).

We expect τ to be a function of the temperature, electron number density, and ion number density of a plasma. Appendix B presents an approximate expression for the electron-ion momentum-transfer collision time in the second Born approximation [Eqs. (B38)–(B43)], which Eq. (16) suggests could be used as an estimate of τ.

Figure 3 plots the electron and ion Pedersen and Hall currents as functions of $\omega_{ce}\tau$ and $\omega_{ci}\tau$, as predicted by the Lorentz-force model. The plots assume $\mathbf{E} = E_x\,\mathbf{e}_x$.

D. Idealized representations of electron and ion trajectories

Figure 4 illustrates idealized electron and ion trajectories in a plasma as predicted by the Lorentz-force model, assuming $\mathbf{E} = E_x\,\mathbf{e}_x$.

Figure 4(a) is an idealized representation of particle trajectories in the collisionless limit ($\omega_{ce}\tau \to \infty$, $\omega_{ci}\tau \to \infty$).

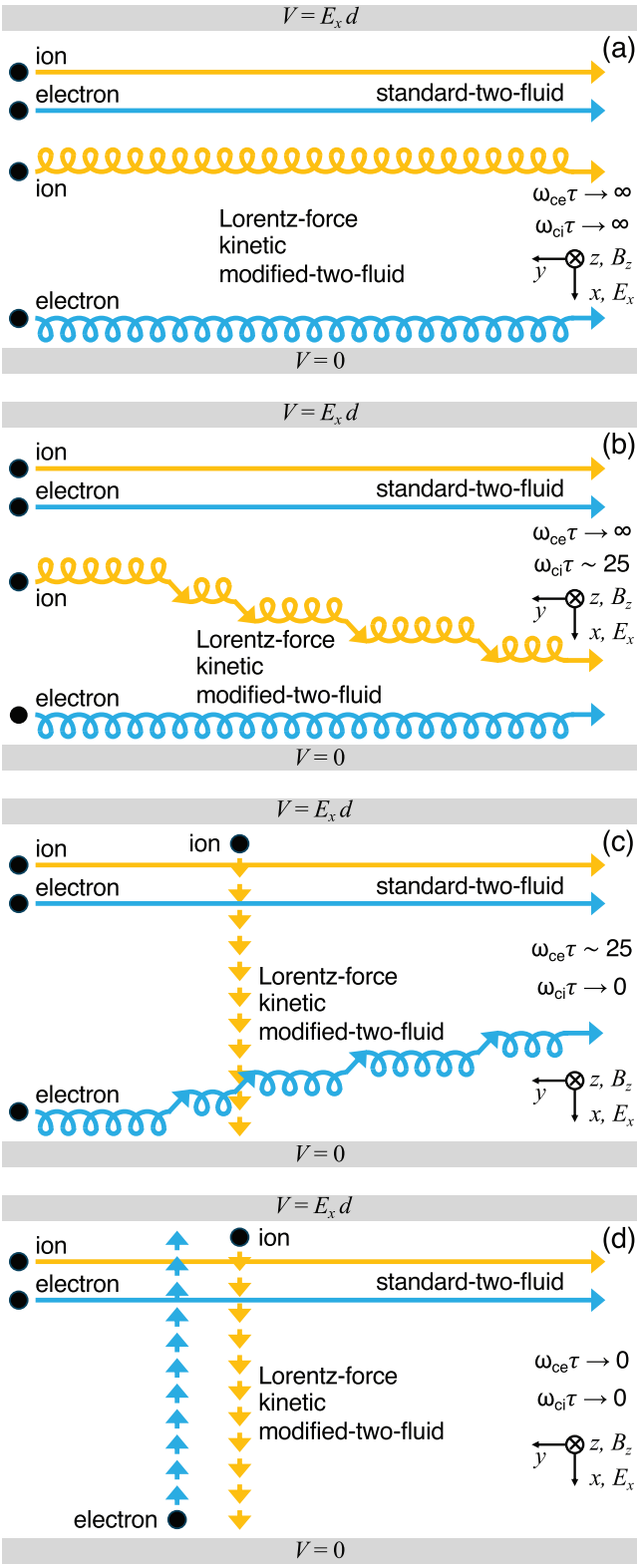


FIG. 4. Idealized steady-state electron and ion trajectories as predicted by the Lorentz-force, kinetic, modified-two-fluid, and standard-two-fluid models of a plasma. The figure assumes $\mathbf{E} = E_x\,\mathbf{e}_x$, $\mathbf{B} = B_z\,\mathbf{e}_z$, and represents four cases. The Lorentz-force, kinetic, and modified-two-fluid models make identical predictions, which differ significantly from those of the standard-two-fluid model. The four models agree in the collisionless limit ($\omega_{ce}\tau \to \infty$, $\omega_{ci}\tau \to \infty$).

In this limit, the Lorentz-force model predicts collisions are so infrequent that, to a good approximation, electrons and ions simply drift in the $\mathbf{E} \times \mathbf{B}$ direction at the $c(\mathbf{E} \times \mathbf{B})/B_z^2 = -(cE_x/B_z)\,\mathbf{e}_y$ velocity.

Figure 4(b) is an idealized representation of particle trajectories when $\omega_{ce}\tau \to \infty$ and $\omega_{ci}\tau \sim 25$. Under these conditions, the Lorentz-force model predicts the electron Pedersen current is negligible, whereas the ion Pedersen current is significant.

Figure 4(c) is an idealized representation of particle trajectories when $\omega_{ce}\tau \sim 25$ and $\omega_{ci}\tau \to 0$. Under these conditions, the Lorentz-force model predicts the electron and ion Pedersen currents are significant, and the ion Hall current is negligible.

Figure 4(d) is an idealized representation of particle trajectories in the collisional limit ($\omega_{ce}\tau \to 0$, $\omega_{ci}\tau \to 0$). In this limit, the Lorentz-force model predicts the interparticle collision frequency is so high that, between collisions, electrons and ions cannot accelerate to velocities sufficiently high to be significantly affected by the magnetic field. The model predicts the electron and ion currents are approximately parallel to $\mathbf{E}$. Hence the model predicts the electron and ion Pedersen currents dominate, and the electron and ion Hall currents are negligible.

III. KINETIC MODEL

A. Electron and ion Boltzmann equations

The kinetic model of a plasma considered by this article is based on the electron and ion Boltzmann equations in the relaxation-time approximation [26]. The electron Boltzmann equation can be expressed as follows:

$$\frac{\partial f_e}{\partial t} + \mathbf{v}\cdot\frac{\partial f_e}{\partial \mathbf{r}} - \frac{e}{m_e}\left(\mathbf{E} + \frac{\mathbf{v}\times\mathbf{B}}{c}\right)\cdot\frac{\partial f_e}{\partial \mathbf{v}} = \left.\frac{\partial f_e}{\partial t}\right|_{\text{collisions}}. \tag{17}$$

The quantity $f_e = f_e\ (t,\ \mathbf{r},\ \mathbf{v})$ is the electron velocity-distribution function, $\mathbf{r} = x\mathbf{e}_x + y\mathbf{e}_y + z\mathbf{e}_z$ is position, and $\mathbf{v} = v_x\,\mathbf{e}_x + v_y\,\mathbf{e}_y + v_z\,\mathbf{e}_z$ is velocity.

Various forms of the collision term that appears on the right-hand side of Eq. (17) have been considered by the literature. One is the Boltzmann collision operator, which models binary collisions [27]. As observed by Krall and Trivelpiece [27], the Boltzmann equation with a Boltzmann collision term "is nearly intractable … both because it is in general nonlinear and also because of the complicated collision integral". In Ref. [28], Rosenbluth, MacDonald, and Judd work with a Fokker-Planck collision term, which can be used to model the cumulative effect of a large number of small deflections caused by long-range Coulomb interactions. As observed by Spitzer [29] (and made clear by Ref. [28]), the "solution of the resultant equation is a matter of some complexity". The original Fokker-Planck collision term ignores magnetic-field effects. Recent publications have developed Fokker-Planck terms that account for the presence of an ambient magnetic field [30–43].

In this article, we do not attempt to develop a collision term that is highly accurate; i.e., one that enables conservation of the total *canonical* momentum of the plasma-electromagnetic-

field system coupled to the external hardware that generates the applied **E** and **B** fields [44,45]. We also neglect momentum loss by charged particles due to cyclotron radiation, bremsstrahlung, etc.

We instead work with the simplest possible collision term that is reasonably accurate. More specifically, we work with the Bhatnagar-Gross-Krook (BGK) collision term [26]:

$$\left.\frac{\partial f_e}{\partial t}\right|_{\text{collisions}} = -\left(\frac{f_e - f_{e0}}{\tau_{ei}}\right), \tag{18}$$

$$f_e = f_{e0} - \tau_{ei}\left.\frac{\partial f_e}{\partial t}\right|_{\text{collisions}} = f_{e0} + f_{e1}, \tag{19}$$

$$f_{e0} = n_e\left(\frac{m_e}{2\pi k_B T}\right)^{3/2}\exp\left(\frac{-m_e\left(v_x^2+v_y^2+v_z^2\right)}{2k_B T}\right). \tag{20}$$

We justify use of the BGK term [Eqs. (18)–(20)] because it is analytically tractable, provides useful physical insight, and appears to give results that are accurate to within a factor of ∼2 over a wide range of plasma parameters.

As suggested by Eq. (18), we assume collisions change the electron distribution function by the amount $f_e - f_{e0}$ on a timescale given by τ_{ei}. As suggested by Eq. (19), we assume f_e is the solution to Eqs. (17)–(18), and is a perturbation to the Maxwell-Boltzmann distribution function f_{e0}, Eq. (20). The quantity τ_{ei} is the electron-ion momentum-transfer collision time, k_B is the Boltzmann constant, and T is the temperature (which we assume to be the same for electrons and ions). We make the simplifying assumption that τ_{ei} can be approximated as a constant.

Equations (17)–(20) can be interpreted as follows. We consider a plasma with no **E** and **B** fields in the steady state at $t = 0$. We assume the initial electron distribution function is given by Eq. (20). When **E** and **B** fields are turned on, we expect the plasma to evolve to a new steady state defined by f_e, on a timescale given by τ_{ei}. When the **E** and **B** fields are subsequently turned off, we expect the plasma to relax back to the Maxwellian given by Eq. (20) on a timescale given by τ_{ei}. These expectations are consistent with the time-dependent currents developed by Sec. IV C.

The ion Boltzmann equation with the BGK collision term can be expressed as follows:

$$\frac{\partial f_i}{\partial t} + \mathbf{v}\cdot\frac{\partial f_i}{\partial \mathbf{r}} + \frac{Ze}{m_i}\left(\mathbf{E} + \frac{\mathbf{v}\times\mathbf{B}}{c}\right)\cdot\frac{\partial f_i}{\partial \mathbf{v}} = \left.\frac{\partial f_i}{\partial t}\right|_{\text{collisions}}, \tag{21}$$

$$\left.\frac{\partial f_i}{\partial t}\right|_{\text{collisions}} = -\left(\frac{f_i - f_{i0}}{\tau_{ie}}\right), \tag{22}$$

$$f_i = f_{i0} - \tau_{ie}\left.\frac{\partial f_i}{\partial t}\right|_{\text{collisions}} = f_{i0} + f_{i1}, \tag{23}$$

$$f_{i0} = n_i\left(\frac{m_i}{2\pi k_B T}\right)^{3/2}\exp\left(\frac{-m_i\left(v_x^2+v_y^2+v_z^2\right)}{2k_B T}\right). \tag{24}$$

The quantity $f_i = f_i\,(t, \mathbf{r}, \mathbf{v})$ is the ion velocity-distribution function. We assume the solution f_i to Eqs. (21)–(24) is a perturbation to the Maxwell-Boltzmann distribution function f_{i0}, and τ_{ie} is the ion-electron momentum-transfer collision time. We make the simplifying assumption that τ_{ie} can be approximated as a constant.

B. Electron and ion conductivity tensors

We begin with Eqs. (17)–(20) and obtain, after some algebra (Appendix B), the following expression for the electron conductivity tensor $\underline{\sigma}_e$:

$$\underline{\sigma}_e = \begin{pmatrix} \frac{\sigma_e}{\left(1+\omega_{ce}^2\tau_{ei}^2\right)} & \frac{-\omega_{ce}\tau_{ei}\sigma_e}{\left(1+\omega_{ce}^2\tau_{ei}^2\right)} & 0 \\ \frac{\omega_{ce}\tau_{ei}\sigma_e}{\left(1+\omega_{ce}^2\tau_{ei}^2\right)} & \frac{\sigma_e}{\left(1+\omega_{ce}^2\tau_{ei}^2\right)} & 0 \\ 0 & 0 & \sigma_e \end{pmatrix}. \tag{25}$$

Equation (25) is identical to Eq. (4), which is derived from the electron Lorentz-force equation.

Since the form of Eqs. (21)–(24) is identical to that of Eqs. (17)–(20) we can, by inspection, write the ion conductivity tensor $\underline{\sigma}_i$:

$$\underline{\sigma}_i = \begin{pmatrix} \frac{\sigma_i}{\left(1+\omega_{ci}^2\tau_{ie}^2\right)} & \frac{\omega_{ci}\tau_{ie}\sigma_i}{\left(1+\omega_{ci}^2\tau_{ie}^2\right)} & 0 \\ \frac{-\omega_{ci}\tau_{ie}\sigma_i}{\left(1+\omega_{ci}^2\tau_{ie}^2\right)} & \frac{\sigma_i}{\left(1+\omega_{ci}^2\tau_{ie}^2\right)} & 0 \\ 0 & 0 & \sigma_i \end{pmatrix}. \tag{26}$$

Equation (26) is identical to Eq. (8), which is derived from the ion Lorentz-force equation.

It is clear the arguments used to derive Eq. (16) also directly apply to the kinetic model. As suggested by Figs. 3 and 4, currents predicted by the Lorentz-force and kinetic models are in agreement.

IV. MODIFIED-TWO-FLUID MODEL

A. Equations of the modified-two-fluid model

In this section we present a modified-two-fluid model of a plasma. We refer to the model as *modified* to distinguish it from the well-known *standard*-two-fluid model outlined by Sec. V.

We derive the modified-two-fluid equations by neglecting spatial gradients in Eqs. (17) and (21), multiplying Eq. (17) by m_e, multiplying Eq. (21) by m_i, then taking the first velocity moment of each of the two equations. This is the procedure normally used to derive fluid equations from Boltzmann equations, as outlined, for example, by Chen [46]:

$$m_e n_e\frac{\partial \mathbf{u}_e}{\partial t} + n_e e\left(\mathbf{E} + \frac{\mathbf{u}_e\times\mathbf{B}}{c}\right) = -\frac{m_e n_e \mathbf{u}_e}{\tau_{ei}}, \tag{27}$$

$$m_i n_i\frac{\partial \mathbf{u}_i}{\partial t} - n_i Ze\left(\mathbf{E} + \frac{\mathbf{u}_i\times\mathbf{B}}{c}\right) = -\frac{m_i n_i \mathbf{u}_i}{\tau_{ie}}. \tag{28}$$

The quantities $\mathbf{u}_e$ and $\mathbf{u}_i$ are the electron and ion fluid velocities, respectively. In the steady state, Eqs. (27) and (28) become

$$n_e e\left(\mathbf{E} + \frac{\mathbf{u}_e\times\mathbf{B}}{c}\right) = -\frac{m_e n_e \mathbf{u}_e}{\tau_{ei}}, \tag{29}$$

$$-n_i Ze\left(\mathbf{E} + \frac{\mathbf{u}_i\times\mathbf{B}}{c}\right) = -\frac{m_i n_i \mathbf{u}_i}{\tau_{ie}}. \tag{30}$$

Equations (29) and (30) are identical to Eqs. (A45) and (A49).

B. Electron and ion conductivity tensors

Equation (29) can be expressed as follows:

$$\mathbf{E} = \underline{\eta}_e \mathbf{j}_e, \tag{31}$$

$$\underline{\eta}_e = \begin{pmatrix} \eta_e & \frac{B_z}{n_e e c} & 0 \\ -\frac{B_z}{n_e e c} & \eta_e & 0 \\ 0 & 0 & \eta_e \end{pmatrix}, \tag{32}$$

$$\eta_e = \frac{m_e}{n_e e^2 \tau_{ei}}, \tag{33}$$

where $\underline{\eta}_e$ is the electron resistivity tensor and η_e is the scalar electron resistivity. Equation (32) is identical to Eq. (A43).

Operating on both sides of Eq. (31) with $\underline{\sigma}_e = \underline{\eta}_e^{-1}$, the inverse of the electron resistivity tensor, we obtain the following:

$$\underline{\sigma}_e \mathbf{E} = \mathbf{j}_e, \tag{34}$$

$$\underline{\sigma}_e = \begin{pmatrix} \frac{\sigma_e}{(1+\omega_{ce}^2\tau_{ei}^2)} & \frac{-\omega_{ce}\tau_{ei}\sigma_e}{(1+\omega_{ce}^2\tau_{ei}^2)} & 0 \\ \frac{\omega_{ce}\tau_{ei}\sigma_e}{(1+\omega_{ce}^2\tau_{ei}^2)} & \frac{\sigma_e}{(1+\omega_{ce}^2\tau_{ei}^2)} & 0 \\ 0 & 0 & \sigma_e \end{pmatrix}. \tag{35}$$

Equation (35) is identical to Eqs. (4) and (25), which are derived from the Lorentz-force and kinetic models, respectively. Equation (29); Eqs. (31)–(32); and Eqs. (34)–(35) are mathematically equivalent.

Beginning with Eq. (30) we obtain a similar set of equations for the ions:

$$\mathbf{E} = \underline{\eta}_i \mathbf{j}_i, \tag{36}$$

$$\underline{\eta}_i = \begin{pmatrix} \eta_i & \frac{-B_z}{n_i Z e c} & 0 \\ \frac{B_z}{n_i Z e c} & \eta_i & 0 \\ 0 & 0 & \eta_i \end{pmatrix}, \tag{37}$$

$$\eta_i = \frac{m_i}{n_i Z^2 e^2 \tau_{ie}}, \tag{38}$$

$$\underline{\sigma}_i \mathbf{E} = \mathbf{j}_i, \tag{39}$$

$$\underline{\sigma}_i = \begin{pmatrix} \frac{\sigma_i}{(1+\omega_{ci}^2\tau_{ie}^2)} & \frac{\omega_{ci}\tau_{ie}\sigma_i}{(1+\omega_{ci}^2\tau_{ie}^2)} & 0 \\ \frac{-\omega_{ci}\tau_{ie}\sigma_i}{(1+\omega_{ci}^2\tau_{ie}^2)} & \frac{\sigma_i}{(1+\omega_{ci}^2\tau_{ie}^2)} & 0 \\ 0 & 0 & \sigma_i \end{pmatrix}. \tag{40}$$

The quantity $\underline{\eta}_i$ is the ion resistivity tensor, and η_i is the scalar ion resistivity. Equation (37) is identical to Eq. (A47); Eq. (40) is identical to Eqs. (8) and (26). Equation (30); Eqs. (36)–(37); and Eqs. (39)–(40) are mathematically equivalent.

It is clear the arguments used to derive Eq. (16) also directly apply to the modified-two-fluid model. As suggested by Figs. 3 and 4, currents predicted by the Lorentz-force, kinetic, and modified-two-fluid models are in agreement.

C. Time-dependent Pedersen, Hall, and Birkeland currents

We include here expressions for time-dependent Pedersen, Hall, and Birkeland currents as derived from Eqs. (27) and (28). The expressions assume $\mathbf{E} = E_x \mathbf{e}_x + E_z \mathbf{e}_z$, and all currents equal 0 at $t = 0$. As expected, the currents evolve to the steady-state values given by Eqs. (34), (35), (39), and (40). In addition, as expected from Eqs. (16), (17), (21), (27), and (28), the currents approach their steady-state values with a time constant given by τ [Eq. (16)].

The time-dependent electron Pedersen, Hall, and Birkeland currents can be expressed as follows:

$$j_{ex} = -n_e e u_{ex} = -n_e e \Big[(\alpha_e \cos(\omega_{ce} t) + \beta_e \sin(\omega_{ce} t)) \exp\left(-\frac{t}{\tau}\right) - \alpha_e \Big], \tag{41}$$

$$j_{ey} = -n_e e u_{ey} = -n_e e \Big[(\alpha_e \sin(\omega_{ce} t) - \beta_e \cos(\omega_{ce} t)) \exp\left(-\frac{t}{\tau}\right) + \beta_e \Big], \tag{42}$$

$$j_{ez} = -n_e e u_{ez} = \frac{n_e e^2 E_z \tau}{m_e} \left(1 - \exp\left(-\frac{t}{\tau}\right)\right), \tag{43}$$

$$\alpha_e = \frac{1}{(1+\omega_{ce}^2\tau^2)} \left(\frac{e E_x \tau}{m_e}\right), \tag{44}$$

$$\beta_e = \frac{-\omega_{ce}^2\tau^2}{(1+\omega_{ce}^2\tau^2)} \left(\frac{c E_x}{B_z}\right). \tag{45}$$

The time-dependent ion Pedersen, Hall, and Birkeland currents are as follows:

$$j_{ix} = n_i Z e u_{ix} = n_i Z e \Big[(\alpha_i \cos(\omega_{ci} t) + \beta_i \sin(\omega_{ci} t)) \exp\left(-\frac{t}{\tau}\right) - \alpha_i \Big], \tag{46}$$

$$j_{iy} = n_i Z e u_{iy} = -n_i Z e \Big[(\alpha_i \sin(\omega_{ci} t) - \beta_i \cos(\omega_{ci} t)) \exp\left(-\frac{t}{\tau}\right) + \beta_i \Big], \tag{47}$$

$$j_{iz} = n_i Z e u_{iz} = \frac{n_i Z^2 e^2 E_z \tau}{m_i} \left(1 - \exp\left(-\frac{t}{\tau}\right)\right), \tag{48}$$

$$\alpha_i = \frac{-1}{(1+\omega_{ci}^2\tau^2)} \left(\frac{Z e E_x \tau}{m_i}\right), \tag{49}$$

$$\beta_i = \frac{\omega_{ci}^2\tau^2}{(1+\omega_{ci}^2\tau^2)} \left(\frac{c E_x}{B_z}\right). \tag{50}$$

V. STANDARD-TWO-FLUID MODEL

A. Equations of the standard-two-fluid model

We begin with the standard-two-fluid momentum equations as they usually appear in the literature [29,46–49], and assume spatial gradients can be neglected:

$$m_e n_e \frac{\partial \mathbf{u}_e}{\partial t} + n_e e\left(\mathbf{E} + \frac{\mathbf{u}_e \times \mathbf{B}}{c}\right) = \mathbf{P}_{ei}, \tag{51}$$

$$m_i n_i \frac{\partial \mathbf{u}_i}{\partial t} - n_i Ze\left(\mathbf{E} + \frac{\mathbf{u}_i \times \mathbf{B}}{c}\right) = \mathbf{P}_{ie}, \tag{52}$$

$$\mathbf{P}_{ei} = -\mathbf{P}_{ie}, \tag{53}$$

$$\mathbf{P}_{ei} = \frac{m_e n_e}{\tau_{ei}}(\mathbf{u}_i - \mathbf{u}_e) = -\frac{m_i n_i}{\tau_{ie}}(\mathbf{u}_e - \mathbf{u}_i), \tag{54}$$

$$\mathbf{P}_{ie} = -\frac{m_e n_e}{\tau_{ei}}(\mathbf{u}_i - \mathbf{u}_e) = \frac{m_i n_i}{\tau_{ie}}(\mathbf{u}_e - \mathbf{u}_i). \tag{55}$$

The quantity $\mathbf{P}_{ei}$ is the electron-kinetic-momentum density transferred to ion-kinetic-momentum density per unit time due to collisions; $\mathbf{P}_{ie}$ is similarly defined.

Equations (51), (52), (54), and (55) can be obtained by taking the first velocity moment of each of the following two Boltzmann equations, neglecting spatial gradients, and invoking Eq. (53), as demonstrated by Ref. [50]:

$$\frac{\partial f_e}{\partial t} + \mathbf{v}\cdot\frac{\partial f_e}{\partial \mathbf{r}} - \frac{e}{m_e}\left(\mathbf{E} + \frac{\mathbf{v}\times\mathbf{B}}{c}\right)\cdot\frac{\partial f_e}{\partial \mathbf{v}} = -\left(\frac{f_e - f_i}{\tau_{ei}}\right), \tag{56}$$

$$\frac{\partial f_i}{\partial t} + \mathbf{v}\cdot\frac{\partial f_i}{\partial \mathbf{r}} + \frac{Ze}{m_i}\left(\mathbf{E} + \frac{\mathbf{v}\times\mathbf{B}}{c}\right)\cdot\frac{\partial f_i}{\partial \mathbf{v}} = -\left(\frac{f_i - f_e}{\tau_{ie}}\right). \tag{57}$$

Equations (51), (52), (54), and (55) can also be obtained from a linearized version of the Fokker-Planck term [47,51].

Equations (51)–(55) can be combined to obtain the following:

$$m_e n_e \frac{\partial \mathbf{u}_e}{\partial t} + n_e e\left(\mathbf{E} + \frac{\mathbf{u}_e \times \mathbf{B}}{c}\right) = \frac{m_e n_e}{\tau_{ei}}(\mathbf{u}_i - \mathbf{u}_e), \tag{58}$$

$$m_i n_i \frac{\partial \mathbf{u}_i}{\partial t} - n_i Ze\left(\mathbf{E} + \frac{\mathbf{u}_i \times \mathbf{B}}{c}\right) = -\frac{m_e n_e}{\tau_{ei}}(\mathbf{u}_i - \mathbf{u}_e). \tag{59}$$

It is useful to separate the electron and ion fluid velocities into components perpendicular and parallel to the magnetic field:

$$\mathbf{u}_e = \mathbf{u}_{e\perp} + \mathbf{u}_{e\parallel}, \tag{60}$$

$$\mathbf{u}_i = \mathbf{u}_{i\perp} + \mathbf{u}_{i\parallel}. \tag{61}$$

Combining Eqs. (58)–(61) we obtain the following:

$$m_e n_e \frac{\partial \mathbf{u}_{e\perp}}{\partial t} + n_e e\left(\mathbf{E}_\perp + \frac{\mathbf{u}_{e\perp} \times \mathbf{B}}{c}\right) = \frac{m_e n_e}{\tau_{ei}}(\mathbf{u}_{i\perp} - \mathbf{u}_{e\perp}), \tag{62}$$

$$m_e n_e \frac{\partial \mathbf{u}_{e\parallel}}{\partial t} + n_e e\mathbf{E}_\parallel = \frac{m_e n_e}{\tau_{ei}}(\mathbf{u}_{i\parallel} - \mathbf{u}_{e\parallel}), \tag{63}$$

$$m_i n_i \frac{\partial \mathbf{u}_{i\perp}}{\partial t} - n_i Ze\left(\mathbf{E}_\perp + \frac{\mathbf{u}_{i\perp} \times \mathbf{B}}{c}\right) = -\frac{m_e n_e}{\tau_{ei}}(\mathbf{u}_{i\perp} - \mathbf{u}_{e\perp}), \tag{64}$$

$$m_i n_i \frac{\partial \mathbf{u}_{i\parallel}}{\partial t} - n_i Ze\mathbf{E}_\parallel = -\frac{m_e n_e}{\tau_{ei}}(\mathbf{u}_{i\parallel} - \mathbf{u}_{e\parallel}). \tag{65}$$

In the steady state

$$n_e e\left(\mathbf{E}_\perp + \frac{\mathbf{u}_{e\perp} \times \mathbf{B}}{c}\right) = \frac{m_e n_e}{\tau_{ei}}(\mathbf{u}_{i\perp} - \mathbf{u}_{e\perp}), \tag{66}$$

$$n_e e\mathbf{E}_\parallel = \frac{m_e n_e}{\tau_{ei}}(\mathbf{u}_{i\parallel} - \mathbf{u}_{e\parallel}), \tag{67}$$

$$-n_i Ze\left(\mathbf{E}_\perp + \frac{\mathbf{u}_{i\perp} \times \mathbf{B}}{c}\right) = -\frac{m_e n_e}{\tau_{ei}}(\mathbf{u}_{i\perp} - \mathbf{u}_{e\perp}), \tag{68}$$

$$-n_i Ze\mathbf{E}_\parallel = -\frac{m_e n_e}{\tau_{ei}}(\mathbf{u}_{i\parallel} - \mathbf{u}_{e\parallel}). \tag{69}$$

B. Electron and ion conductivity tensors when B ≠ 0

We first consider the case with a nonzero magnetic field. According to Eqs. (14), (66), and (68),

$$(\mathbf{u}_{e\perp} - \mathbf{u}_{i\perp}) \times \mathbf{B} = 0. \tag{70}$$

Since we have assumed $\mathbf{B} \neq 0$,

$$(\mathbf{u}_{e\perp} - \mathbf{u}_{i\perp}) = 0. \tag{71}$$

Combining Eqs. (66), (68), and (71) we find that the collision terms vanish:

$$n_e e\left(\mathbf{E}_\perp + \frac{\mathbf{u}_{e\perp} \times \mathbf{B}}{c}\right) = 0, \tag{72}$$

$$n_i Ze\left(\mathbf{E}_\perp + \frac{\mathbf{u}_{i\perp} \times \mathbf{B}}{c}\right) = 0. \tag{73}$$

According to Eqs. (72) and (73), the transverse electron and ion fluid velocities both become the ideal collisionless $c(\mathbf{E}\times\mathbf{B})/B_z^2$ values in the steady state, no matter how short the time between particle collisions:

$$\mathbf{u}_{e\perp} = \frac{c\mathbf{E}\times\mathbf{B}}{B_z^2}, \tag{74}$$

$$\mathbf{u}_{i\perp} = \frac{c\mathbf{E}\times\mathbf{B}}{B_z^2}. \tag{75}$$

The standard-two-fluid model predicts that, in the steady state, the electron and ion fluid velocities are *identical*, independent of $\omega_{ce}\tau_{ei}$ and $\omega_{ci}\tau_{ie}$. It is straightforward to show that in the steady state, Eqs. (51)–(52) lead to Eq. (71) when $\mathbf{B} \neq 0$, independent of the form of the collision terms $\mathbf{P}_{ei}$ and $\mathbf{P}_{ie}$, as long as Eq. (53) is assumed.

As suggested by Eqs. (74) and (75), the standard-two-fluid model predicts that, in the steady state, the plasma achieves perfect magnetic insulation; i.e., that collisions do not result in charged-particle transport in the direction of **E** transverse to **B,** no matter how short the time between collisions. In other words, the model predicts steady-state electron and ion Pedersen currents are identically 0, independent of the time between collisions. In addition, the model predicts that, in the steady state, electron and ion Hall velocities achieve their ideal collisionless values, Eqs. (74) and (75), independent of

the interparticle collision time. In the presence of collisions, it appears the standard-two-fluid model underpredicts the electron and ion Pedersen currents, and overpredicts the electron and ion Hall currents.

It is clear the standard-two-fluid model is inconsistent with the Lorentz-force, kinetic, and modified-two-fluid models outlined by Secs. II, III, and IV, respectively. The standard-two-fluid equations are also inconsistent with elementary physical considerations. For example, we expect that at a sufficiently high collision frequency, charged particles would be unable to accelerate between collisions to a velocity sufficiently high to be significantly affected by the magnetic field. We expect that in the collisional limit, charged particles would drift approximately parallel to $\mathbf{E}$, as indicated by Eqs. (A37) and (A38), and not in the direction of $\mathbf{E}\times\mathbf{B}$.

Combining Eqs. (14), (63), and (65), and assuming $\mathbf{u}_{e||} = \mathbf{u}_{i||} = 0$ at $t = 0$, we find that kinetic momentum parallel to $\mathbf{B}$ is conserved, and obtain the following in the steady state:

$$\mathbf{u}_{e\|} = \frac{-e\mathbf{E}_\| \tau_{ei}}{m_e\left(1+\frac{Zm_e}{m_i}\right)}, \tag{76}$$

$$\mathbf{u}_{i\|} = \frac{Ze\mathbf{E}_\| \tau_{ei}}{m_i\left(1+\frac{Zm_e}{m_i}\right)}. \tag{77}$$

Equations (74)–(77) suggest the electron and ion electrical-conductivity tensors can be expressed as follows:

$$\underline{\sigma}_e = \begin{pmatrix} 0 & \frac{-n_e ec}{B_z} & 0 \\ \frac{n_e ec}{B_z} & 0 & 0 \\ 0 & 0 & \frac{n_e e^2\tau_{ei}}{m_e\left(1+\frac{Zm_e}{m_i}\right)} \end{pmatrix}, \tag{78}$$

$$\underline{\sigma}_i = \begin{pmatrix} 0 & \frac{n_i Zec}{B_z} & 0 \\ \frac{-n_i Zec}{B_z} & 0 & 0 \\ 0 & 0 & \frac{n_i Z^2 e^2\tau_{ei}}{m_i\left(1+\frac{Zm_e}{m_i}\right)} \end{pmatrix}, \tag{79}$$

Combining (54), (55), (78), and (79), we find

$$\tau_{ie} = \frac{m_i \tau_{ei}}{Zm_e}, \tag{80}$$

$$\underline{\sigma}_e = \begin{pmatrix} 0 & \frac{-n_e ec}{B_z} & 0 \\ \frac{n_e ec}{B_z} & 0 & 0 \\ 0 & 0 & \frac{n_e e^2\tau_{ie}}{m_e\left(1+\frac{m_i}{Zm_e}\right)} \end{pmatrix}, \tag{81}$$

$$\underline{\sigma}_i = \begin{pmatrix} 0 & \frac{n_i Zec}{B_z} & 0 \\ \frac{-n_i Zec}{B_z} & 0 & 0 \\ 0 & 0 & \frac{n_i Z^2 e^2\tau_{ie}}{m_i\left(1+\frac{m_i}{Zm_e}\right)} \end{pmatrix}. \tag{82}$$

Equation (80) is significantly different than Eq. (16). However, Eqs. (78)–(82) suggest it would be useful to define *effective* electron-ion and ion-electron collision times:

$$\tau_{ei,\text{effective}} = \frac{\tau_{ei}}{\left(1+\frac{Zm_e}{m_i}\right)}, \tag{83}$$

$$\tau_{ie,\text{effective}} = \frac{\tau_{ie}}{\left(1+\frac{m_i}{Zm_e}\right)} = \frac{\tau_{ei}}{\left(1+\frac{Zm_e}{m_i}\right)}. \tag{84}$$

Hence

$$\tau_{ie,\,\text{effective}} = \tau_{ei,\,\text{effective}} = \tau_{\text{effective}}. \tag{85}$$

Equation (85) is consistent with Eq. (16). When $Zm_e \ll m_i$, then

$$\tau \approx \tau_{\text{effective}}. \tag{86}$$

Combining Eqs. (78)–(85) we obtain the following expressions:

$$\underline{\sigma}_e = \begin{pmatrix} 0 & \frac{-n_e ec}{B_z} & 0 \\ \frac{n_e ec}{B_z} & 0 & 0 \\ 0 & 0 & \sigma_{e,\text{effective}} \end{pmatrix}, \tag{87}$$

$$\underline{\sigma}_i = \begin{pmatrix} 0 & \frac{n_i Zec}{B_z} & 0 \\ \frac{-n_i Zec}{B_z} & 0 & 0 \\ 0 & 0 & \sigma_{i,\text{effective}} \end{pmatrix}, \tag{88}$$

$$\sigma_{e,\text{effective}} = \frac{n_e e^2 \tau_{\text{effective}}}{m_e}, \tag{89}$$

$$\sigma_{i,\text{effective}} = \frac{n_i Z^2 e^2 \tau_{\text{effective}}}{m_i}. \tag{90}$$

The conductivity tensors obtained with the standard-two-fluid model, Eqs. (87) and (88), are independent of $\omega_{ce}\tau$ and $\omega_{ci}\tau$. Hence Eqs. (87) and (88) are inconsistent with the tensors derived from the steady-state Lorentz-force, kinetic, and modified-two-fluid models.

Figure 3 plots electron and ion Pedersen and Hall currents as functions of $\omega_{ce}\tau$ and $\omega_{ci}\tau$, as predicted by the Lorentz-force, kinetic, modified-two-fluid, and standard-two-fluid models. As suggested by the figure, the Lorentz-force, kinetic, and modified-two-fluid models are consistent with the standard-two-fluid model only in the collisionless limit ($\omega_{ce}\tau \to \infty$, $\omega_{ci}\tau \to \infty$) when $\mathbf{B} \neq 0$.

Figure 4 is an idealized representation of electron and ion trajectories for several values of $\omega_{ce}\tau$ and $\omega_{ci}\tau$. As suggested by the figure, the standard-two-fluid model predicts that, in the steady state, the electron and ion Pedersen currents are identically 0, and the electron and ion Hall currents dominate, even when the time between collisions is much less than the particle gyroperiods. These predictions are inconsistent with those of the other three models, and elementary physical considerations.

C. Electron and ion conductivity tensors when B = 0

When $\mathbf{B} = 0$, and $\mathbf{u}_e = \mathbf{u}_i = 0$ at $t = 0$, Eqs. (62)–(65) demonstrate that kinetic momentum is conserved, and the

electron and ion fluid velocities are parallel to **E**:

$$\mathbf{u}_e = \frac{-e\mathbf{E}\tau_{ei}}{m_e\left(1+\frac{Zm_e}{m_i}\right)}, \tag{91}$$

$$\mathbf{u}_i = \frac{Ze\mathbf{E}\tau_{ei}}{m_i\left(1+\frac{Zm_e}{m_i}\right)}. \tag{92}$$

The electron and ion conductivity tensors become scalars:

$$\underline{\sigma}_e = \begin{pmatrix} \sigma_{e,\text{effective}} & 0 & 0 \\ 0 & \sigma_{e,\text{effective}} & 0 \\ 0 & 0 & \sigma_{e,\text{effective}} \end{pmatrix}, \tag{93}$$

$$\underline{\sigma}_i = \begin{pmatrix} \sigma_{i,\text{effective}} & 0 & 0 \\ 0 & \sigma_{i,\text{effective}} & 0 \\ 0 & 0 & \sigma_{i,\text{effective}} \end{pmatrix}. \tag{94}$$

When $\mathbf{B} = 0$, the conductivity tensors derived from the standard-two-fluid model agree with those obtained from the Lorentz-force, kinetic, and modified-two-fluid models in the limit $(Zm_e/m_i) \to 0$.

VI. TIME-DEPENDENT FLUID VELOCITIES PREDICTED BY THE MODIFIED- AND STANDARD-TWO-FLUID MODELS

It is of interest to consider the time evolution of the currents that flow within a plasma subject to electric and magnetic fields. In this section we compare time-dependent fluid velocities as predicted by the modified- and standard-two-fluid models. Equations (41)–(50) are analytic expressions for time-dependent velocities as predicted by the modified-two-fluid model. In this section we make the simplifying assumption that $\mathbf{E} = E_x\,\mathbf{e}_x$ and hence do not use Eqs. (43) and (48). We use the fourth-order Runge-Kutta numerical-integration technique to obtain time-dependent velocities as predicted by the standard-two-fluid model, Eqs. (62) and (64).

Results are plotted by Figs. 5–8, which assume the following:

$$Z = 1, \tag{95}$$

$$m_i = 10m_e, \tag{96}$$

$$\mathbf{E} = E_x\mathbf{e}_x = 3.33\ \text{statvolts/cm}, \tag{97}$$

$$\tau = \tau_{ei} = 2.28\ \text{ps}. \tag{98}$$

Equation (96) facilitates numerical integration of Eqs. (62) and (64).

Two cases are considered by Figs. 5–8:

$$\mathbf{B} = B_z\mathbf{e}_z = 10\ \text{kG}, \tag{99}$$

$$\omega_{ce}\tau = 0.4,\ \omega_{ci}\tau = 0.04, \tag{100}$$

and

$$\mathbf{B} = B_z\mathbf{e}_z = 100\ \text{kG}, \tag{101}$$

$$\omega_{ce}\tau = 4,\ \omega_{ci}\tau = 0.4. \tag{102}$$

Figures 5–8 assume the **E** and **B** fields are turned on at $t = 0$.

As indicated by the figures, the modified- and standard-two-fluid-models agree early in time for all values of $\omega_{ce}\tau$ and $\omega_{ci}\tau$. However, as indicated by Figs. 5 and 7, the standard-two-fluid model predicts u_{ex} and u_{ix} approach 0 in the steady state, which is infinitely less than the steady-state values of u_{ex} and u_{ix} predicted by the modified-two-fluid model.

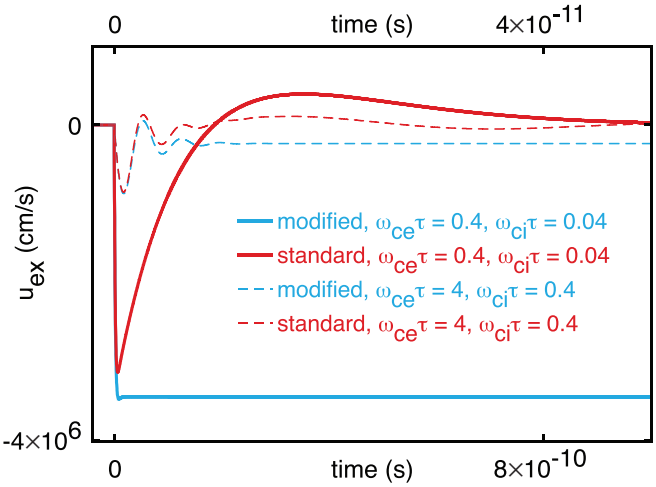


FIG. 5. Time-dependent electron-fluid velocity u_{ex}. The velocity is plotted for the modified- and standard-two-fluid models for two cases: $\omega_{ce}\tau = 0.4$, $\omega_{ci}\tau = 0.04$ (lower time axis) and $\omega_{ce}\tau = 4$, $\omega_{ci}\tau = 0.4$ (upper time axis). The plots assume the electric and magnetic fields are turned on at $t = 0$. The modified- and standard-two-fluid predictions diverge with time. For both cases, the standard-two-fluid model predicts u_{ex} approaches 0 in the steady state, which is infinitely less than the predictions of the modified-two-fluid model.

Since $\omega_{ce}\tau < 1$ for the first case and $\omega_{ce}\tau > 1$ for the second, Fig. 6 finds that the modified- and standard-fluid-model predictions for u_{ey} diverge for the first case but are comparable for the second. Since $\omega_{ci}\tau < 1$ for both cases, Fig. 8 finds

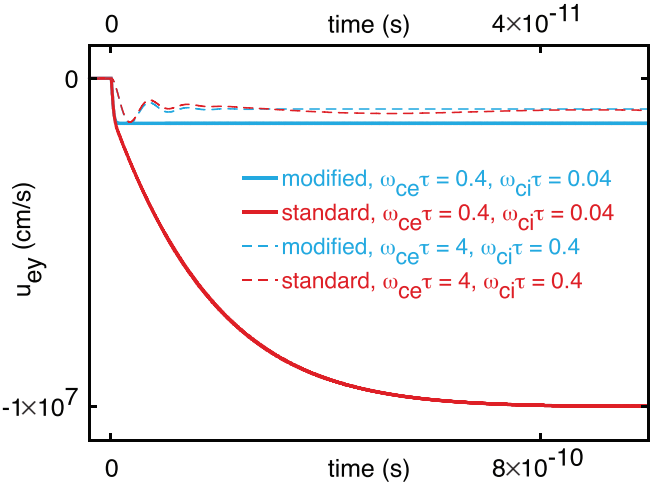


FIG. 6. Time-dependent electron-fluid velocity u_{ey}. The velocity is plotted for the modified- and standard two-fluid models for two cases: $\omega_{ce}\tau = 0.4$, $\omega_{ci}\tau = 0.04$ (lower time axis) and $\omega_{ce}\tau = 4$, $\omega_{ci}\tau = 0.4$ (upper time axis). The plots assume the electric and magnetic fields are turned on at $t = 0$. For the first case, the modified- and standard-two-fluid predictions diverge with time. For the second case, the two predictions are comparable, since $\omega_{ce}\tau$ is significantly larger than 1.

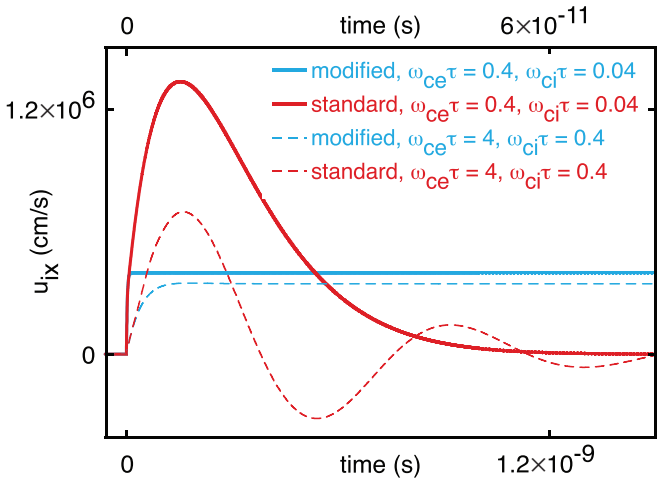


FIG. 7. Time-dependent ion-fluid velocity u_{ix}. The velocity is plotted for the modified- and standard-two-fluid models for two cases: $\omega_{ce}\tau = 0.4$, $\omega_{ci}\tau = 0.04$ (lower time axis) and $\omega_{ce}\tau = 4$, $\omega_{ci}\tau = 0.4$ (upper time axis). The plots assume the electric and magnetic fields are turned on at $t = 0$. The modified- and standard-two-fluid predictions diverge with time. For both cases, the standard-two-fluid model predicts u_{ix} approaches 0 in the steady state, which is infinitely less than the predictions of the modified-two-fluid model.

that, for both cases, the modified- and standard-fluid-model predictions for u_{iy} diverge.

VII. ADDITIONAL COMMENTS ON THE STANDARD-TWO-FLUID MODEL

A. Ion-rest frame

According to Eqs. (74) and (75), which represent the standard-two-fluid model in the steady state in the *laboratory* frame, the ion rest frame is the same as the electron rest frame when $\mathbf{B} \neq 0$. Hence in this frame in the steady state, $\mathbf{u}_i = \mathbf{u}_e = \mathbf{j}_i = \mathbf{j}_e = \mathbf{E} = 0$.

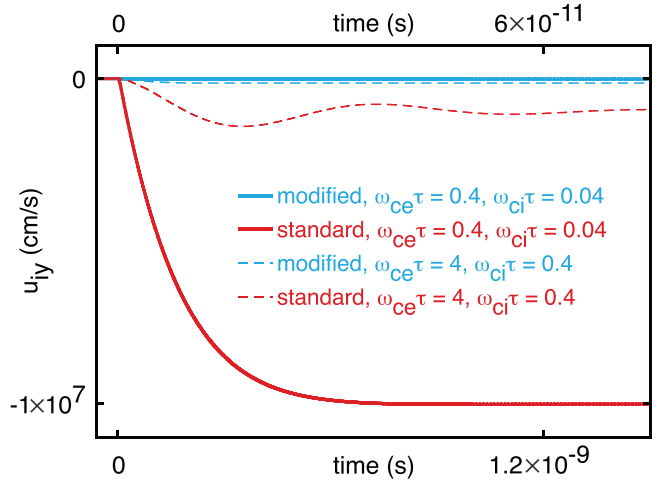


FIG. 8. Time-dependent ion-fluid velocity u_{iy}. The velocity is plotted for the modified- and standard-two-fluid models for two cases: $\omega_{ce}\tau = 0.4$, $\omega_{ci}\tau = 0.04$ (lower time axis) and $\omega_{ce}\tau = 4$, $\omega_{ci}\tau = 0.4$ (upper time axis). The plots assume the electric and magnetic fields are turned on at $t = 0$. The modified- and standard-two-fluid predictions diverge with time, since for both cases, $\omega_{ci}\tau < 1$.

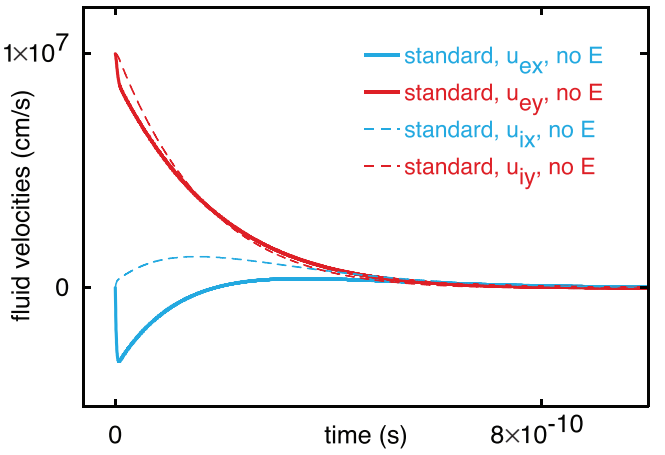


FIG. 9. Time-dependent electron- and ion-fluid velocities as predicted by the standard-two-fluid model. The plots assume $\mathbf{E} = 0$, $\mathbf{B} = 10\,\mathrm{kG}$, $\omega_{ce}\tau = 0.4$, $\omega_{ci}\tau = 0.04$, the initial values of $\mathbf{u}_{ex} = \mathbf{u}_{ix} = 0$, and the initial values of $\mathbf{u}_{ey} = \mathbf{u}_{iy} = 10^7\,\mathrm{cm/s}$. Several authors suggest the collision terms of the standard-two-fluid model conserve kinetic momentum; however, the plots suggest kinetic momentum is not always conserved.

We observe that Braginskii [47] and Epperlein and Haines [51] calculate electron conductivity tensors in the ion rest frame in the steady state. However, as indicated above, the standard-two-fluid model predicts that the ion rest frame is the same as the electron rest frame, and $\mathbf{u}_i = \mathbf{u}_e = \mathbf{j}_i = \mathbf{j}_e = \mathbf{E} = 0$ in the ion-and-electron rest frame in the steady state.

B. Conservation of kinetic momentum

We consider a plasma with $\mathbf{E} = 0$, $\mathbf{B} = 10\,\mathrm{kG}$, and solve numerically Eqs. (62) and (64) of the standard-two-fluid model. We assume Eqs. (95), (96), and (98), and the following initial values for the fluid velocities:

$$\mathbf{u}_{ex} = \mathbf{u}_{ix} = 0, \tag{103}$$

$$\mathbf{u}_{ey} = \mathbf{u}_{iy} = 10^7\ \mathrm{cm/s}. \tag{104}$$

The four velocities evolve with time as plotted by Fig. 9.

The only dissipative terms in Eqs. (62) and (64) are the collision terms of the standard-two-fluid model. Several authors suggest these terms conserve *kinetic* momentum; i.e., that the terms guarantee that kinetic momentum transferred by collisions from electrons to ions is equal and opposite to that transferred from ions to electrons. However, Fig. 9 makes clear that, for the case considered, the initial kinetic momentum of the particles dissipates completely and is not conserved.

It is well known that charged particles do not conserve *kinetic* momentum when subject to the $\mathbf{v} \times \mathbf{B}$ force; i.e., when charged particles have velocity components perpendicular to $\mathbf{B}$. (For example, a single collisionless electron gyrating in a magnetic field does not conserve kinetic momentum.) However, we note that the collision terms of the standard-two-fluid equations conserve kinetic momentum when $\mathbf{B} = 0$.

VIII. SUMMARY

We have derived explicit analytic expressions for electron and ion electrical-conductivity tensors from Lorentz-force, kinetic, and *modified*-two-fluid models of a plasma. Even though the derivations (Appendices A, B, and Sec. IV) differ significantly, the tensors derived from the three models are identical. In both the collisionless ($\omega_{ce}\tau \to \infty$, $\omega_{ci}\tau \to \infty$) and collisional ($\omega_{ce}\tau \to 0$, $\omega_{ci}\tau \to 0$) limits, the tensors predict electron and ion Pedersen, Hall, and Birkeland currents that are consistent with elementary physical considerations.

We have also derived electron and ion conductivity tensors from the *standard*-two-fluid model of a plasma. The tensors predict that in the steady state, a plasma achieves perfect magnetic insulation; i.e., that collisions do not result in charged-particle drifts in the direction of **E** that is transverse to **B,** no matter how short the time between collisions. The tensors also predict that, in the steady state, electrons and ions both drift at the ideal $\mathbf{E}\times\mathbf{B}$ velocity in the ideal $\mathbf{E}\times\mathbf{B}$ direction, no matter how short the time between collisions.

The vanishing electron and ion Pedersen currents are inconsistent with the physical expectation that collisions would allow charged-particle transport across a magnetic field. The vanishing Pedersen currents are infinitely less than those predicted by the Lorentz-force, kinetic, and modified-two-fluid models in the presence of collisions. In addition, the ideal Hall velocities diverge from the Hall velocities that are predicted by the Lorentz-force, kinetic, and modified-two-fluid models in the collisional limit ($\omega_{ce}\tau \to 0$, $\omega_{ci}\tau \to 0$). These discrepancies are caused by the collision terms of the standard-two-fluid model.

Nevertheless, it is clear the standard-two-fluid model is, for some applications, more useful than the Lorentz-force, kinetic, and modified-two-fluid models. As indicated by Figs. 3 and 4, the standard-two-fluid model is consistent, in the steady state, with the Lorentz-force, kinetic, and modified-two-fluid models in the collisionless limit ($\omega_{ce}\tau \to \infty$, $\omega_{ci}\tau \to \infty$). As suggested by Eqs. (93), (94), (A37), and (A38), the standard-two-fluid model is consistent, in the steady state, with the Lorentz-force, kinetic, and modified-two-fluid models when $\mathbf{B} = 0$ and ($Zm_e/m_i \to 0$). As indicated by Figs. 5–8, time-dependent currents simulated by the modified- and standard-two-fluid models agree early in time, for all values of $\omega_{ce}\tau$ and $\omega_{ci}\tau$.

ACKNOWLEDGMENTS

The authors are immensely grateful to the following colleagues for critical discussions and sustained support: Tom Arsenlis, Saeed Assadi, Cuyler Beatty, Farhat Beg, Dan Behne, E. Michael Campbell, Jim Chang, Chris Cooper, John Cortes, John Edwards, Lee Ellison, Jennifer Ellsworth, David Fehl, Glenn Gerdin, Gary Grim, Jason Hamilton, Jim Hammer, Ken Heinz, Mark Herrmann, Trevor Hutchinson, Brian Hutsel, Anagha Iyengar, Jay Javedani, Dan Jobe, Anthony Johnson, Keith LeChien, Ray Leeper, Tony Link, Harry McLean, Donn McMahon, Nathan Meezan, Robin Miles, Nate Pogue, John Porter, Kumar Raman, David Rose, Edl Schamiloglu, Andrea Schmidt, Paul Schmit, Ralph Schneider, Jason Sears, Robert Sharpe, Mike Sheehy, Bryan Sims, Rick Spielman, Richard Town, Katherine Velas, Jim Watson, Adam White, and Andrew Young. The authors are also immensely grateful to our many other colleagues at the following organizations for invaluable contributions: Lawrence Livermore National Laboratory, Voss Scientific, Pacific Fusion, Sandia National Laboratories, and the National Nuclear Security Administration. This work was performed under the auspices of the U.S. Department of Energy by Lawrence Livermore National Laboratory under Contract DE-AC52-07NA27344.

DATA AVAILABILITY

The data that support the findings of this article are not publicly available. The data are available from the authors upon reasonable request.

APPENDIX A: DERIVATION OF CONDUCTIVITY TENSORS, RESISTIVITY TENSORS, AND FLUID EQUATIONS FROM THE LORENTZ-FORCE EQUATIONS

1. Electron and ion conductivity tensors

In this Appendix, we derive general expressions for the electron and ion electrical-conductivity tensors from the Lorentz-force equations, Eqs. (1) and (2). The derivation closely follows those given by Parks [23] and Piel [24]. The derivations by Parks and Piel assume the probability distribution of random collisions as described by Feynman [25].

We first consider an electron within a fully ionized two-component plasma. We assume $\mathbf{E} = E_x\,\mathbf{e}_x + E_y\,\mathbf{e}_y + E_z\,\mathbf{e}_z$ and $\mathbf{B} = B_z\,\mathbf{e}_z$. Hence we can expand Eq. (1) as follows:

$$m_e\frac{dv_{ex}}{dt} = -eE_x - \frac{e}{c}v_{ey}B_z, \tag{A1}$$

$$m_e\frac{dv_{ey}}{dt} = -eE_y + \frac{e}{c}v_{ex}B_z, \tag{A2}$$

$$m_e\frac{dv_{ez}}{dt} = -eE_z. \tag{A3}$$

We assume the electron begins, on average, with 0 velocity:

$$v_{ex}(t=0) = 0, \tag{A4}$$

$$v_{ey}(t=0) = 0, \tag{A5}$$

$$v_{ez}(t=0) = 0. \tag{A6}$$

Equations (A1)–(A6) give the electron velocity as a function of time:

$$v_{ex} = -\frac{cE_x}{B_z}\sin(\omega_{ce}t) + \frac{cE_y}{B_z}(1-\cos(\omega_{ce}t)), \tag{A7}$$

$$v_{ey} = -\frac{cE_y}{B_z}\sin(\omega_{ce}t) - \frac{cE_x}{B_z}(1-\cos(\omega_{ce}t)), \tag{A8}$$

$$v_{ez} = -\frac{eE_z}{m_e}t, \tag{A9}$$

$$\omega_{ce} = \frac{eB_z}{m_e c}. \tag{A10}$$

We define $p(t)$ to be, at time t, the probability an electron suffers a collision per unit time. Hence

$$\int_0^\infty p(t)dt = 1. \tag{A11}$$

We assume collisions occur randomly in time; hence we assume an incremental change in the probability dp is proportional to dt, in the following manner:

$$\frac{dp}{p} = -\frac{dt}{\tau_{ei}}. \tag{A12}$$

We make the simplifying assumption that τ_{ei} can be approximated as a constant. Consequently,

$$p(t)dt = \frac{1}{\tau_{ei}} \exp\left(-\frac{t}{\tau_{ei}}\right)dt \tag{A13}$$

is the probability a collision occurs between times t and $t + dt$, after no collisions have occurred between times 0 and t.

We define a collision as we do in Sec. II B and Fig. 2: a set of one or more scattering events that combined causes each component of the electron velocity to reinitialize, on average, to 0. Multiplying the probability distribution function [Eq. (A13)] by each of the electron velocity components [Eqs. (A7)–(A9)], and integrating over all time, gives components of the electron fluid velocity $\mathbf{u}_e$:

$$\begin{aligned} u_{ex} &= \frac{-c}{\tau_{ei}B_z}\int_0^\infty \exp\left(-\frac{t}{\tau_{ei}}\right)[E_x \sin(\omega_{ce}t) \\ &\quad - E_y(1-\cos(\omega_{ce}t))]dt \\ &= -\frac{1}{\left(1+\omega_{ce}^2\tau_{ei}^2\right)}\frac{e\tau_{ei}E_x}{m_e} + \frac{\omega_{ce}\tau_{ei}}{\left(1+\omega_{ce}^2\tau_{ei}^2\right)}\frac{e\tau_{ei}E_y}{m_e}, \end{aligned} \tag{A14}$$

$$\begin{aligned} u_{ey} &= \frac{-c}{\tau_{ei}B_z}\int_0^\infty \exp\left(-\frac{t}{\tau_{ei}}\right)[E_y \sin(\omega_{ce}t) \\ &\quad + E_x(1-\cos(\omega_{ce}t))]dt \\ &= -\frac{1}{\left(1+\omega_{ce}^2\tau_{ei}^2\right)}\frac{e\tau_{ei}E_y}{m_e} - \frac{\omega_{ce}\tau_{ei}}{\left(1+\omega_{ce}^2\tau_{ei}^2\right)}\frac{e\tau_{ei}E_x}{m_e}, \end{aligned} \tag{A15}$$

$$u_{ez} = -\left(\frac{eE_z}{\tau_{ei}m_e}\right)\int_0^\infty t\exp\left(-\frac{t}{\tau_{ei}}\right)dt = -\frac{e\tau_{ei}E_z}{m_e}. \tag{A16}$$

Since

$$j_{ex} = -n_e e u_{ex}, \tag{A17}$$

$$j_{ey} = -n_e e u_{ey}, \tag{A18}$$

$$j_{ez} = -n_e e u_{ez}, \tag{A19}$$

the components of the electron current can be obtained directly from Eqs. (A14)–(A19):

$$j_{ex} = \frac{\sigma_e}{\left(1+\omega_{ce}^2\tau_{ei}^2\right)}E_x - \frac{\omega_{ce}\tau_{ei}\sigma_e}{\left(1+\omega_{ce}^2\tau_{ei}^2\right)}E_y, \tag{A20}$$

$$j_{ey} = \frac{\omega_{ce}\tau_{ei}\sigma_e}{\left(1+\omega_{ce}^2\tau_{ei}^2\right)}E_x + \frac{\sigma_e}{\left(1+\omega_{ce}^2\tau_{ei}^2\right)}E_y, \tag{A21}$$

$$j_{ez} = \sigma_e E_z, \tag{A22}$$

$$\sigma_e = \frac{n_e e^2 \tau_{ei}}{m_e}. \tag{A23}$$

The quantities j_{ex}, j_{ey}, and j_{ez} are the electron Pedersen, Hall, and Birkeland currents, respectively. Equations (A20)–(A22) can be expressed alternatively as follows:

$$\mathbf{j}_e = \underline{\sigma}_e \mathbf{E}, \tag{A24}$$

$$\underline{\sigma}_e = \begin{pmatrix} \frac{\sigma_e}{\left(1+\omega_{ce}^2\tau_{ei}^2\right)} & \frac{-\omega_{ce}\tau_{ei}\sigma_e}{\left(1+\omega_{ce}^2\tau_{ei}^2\right)} & 0 \\ \frac{\omega_{ce}\tau_{ei}\sigma_e}{\left(1+\omega_{ce}^2\tau_{ei}^2\right)} & \frac{\sigma_e}{\left(1+\omega_{ce}^2\tau_{ei}^2\right)} & 0 \\ 0 & 0 & \sigma_e \end{pmatrix}. \tag{A25}$$

The above arguments apply equally well to ions:

$$\mathbf{j}_i = \underline{\sigma}_i \mathbf{E}, \tag{A26}$$

$$j_{ix} = n_i Z e u_{ix}, \tag{A27}$$

$$j_{iy} = n_i Z e u_{iy}, \tag{A28}$$

$$j_{iz} = n_i Z e u_{iz}, \tag{A29}$$

$$\underline{\sigma}_i = \begin{pmatrix} \frac{\sigma_i}{\left(1+\omega_{ci}^2\tau_{ie}^2\right)} & \frac{\omega_{ci}\tau_{ie}\sigma_i}{\left(1+\omega_{ci}^2\tau_{ie}^2\right)} & 0 \\ \frac{-\omega_{ci}\tau_{ie}\sigma_i}{\left(1+\omega_{ci}^2\tau_{ie}^2\right)} & \frac{\sigma_i}{\left(1+\omega_{ci}^2\tau_{ie}^2\right)} & 0 \\ 0 & 0 & \sigma_i \end{pmatrix}, \tag{A30}$$

$$\sigma_i = \frac{n_i Z^2 e^2 \tau_{ie}}{m_i}, \tag{A31}$$

$$\omega_{ci} = \frac{ZeB_z}{m_i c}. \tag{A32}$$

2. Electron and ion conductivity tensors in the collisionless limit

By definition, in the collisionless limit, the time interval between interparticle collisions is much greater than the particle gyroperiods; i.e., $\omega_{ce}\tau_{ei} \to \infty$ and $\omega_{ci}\tau_{ie} \to \infty$. In this limit, the electron and ion conductivity tensors, Eqs. (A25) and (A30), reduce to the following:

$$\underline{\sigma}_e = \begin{pmatrix} 0 & \frac{-n_e e c}{B_z} & 0 \\ \frac{n_e e c}{B_z} & 0 & 0 \\ 0 & 0 & \sigma_e \end{pmatrix}, \tag{A33}$$

$$\underline{\sigma}_i = \begin{pmatrix} 0 & \frac{n_i Z e c}{B_z} & 0 \\ \frac{-n_i Z e c}{B_z} & 0 & 0 \\ 0 & 0 & \sigma_i \end{pmatrix}. \tag{A34}$$

For example, when $\mathbf{E} = E_x \mathbf{e}_x$, fluid velocities calculated with Eqs. (A18), (A24), (A26), (A28), (A33), and (A34) are as follows:

$$\mathbf{u}_e = \mathbf{u}_{ey} = -\frac{cE_x}{B_z}\mathbf{e}_y, \tag{A35}$$

$$\mathbf{u}_i = \mathbf{u}_{iy} = -\frac{cE_x}{B_z}\mathbf{e}_y. \tag{A36}$$

As expected, in the collisionless limit ($\omega_{ce}\tau_{ei} \to \infty$, $\omega_{ci}\tau_{ie} \to \infty$), the characteristic time between interparticle collisions is so great that, to a good approximation, both electrons and

ions simply drift in the $\mathbf{E}\times\mathbf{B}$ direction at the $c(\mathbf{E}\times\mathbf{B})/B_z^2$ velocity.

3. Electron and ion conductivity tensors in the collisional limit

By definition, in the collisional limit ($\omega_{ce}\tau_{ei}\to 0$, $\omega_{ci}\tau_{ie}\to 0$), the time between interparticle collisions is much less than the particle gyroperiods. In this limit, the electron and ion conductivity tensors, Eqs. (A25) and (A30), reduce to the following:

$$\underline{\sigma}_e = \begin{pmatrix} \sigma_e & 0 & 0 \\ 0 & \sigma_e & 0 \\ 0 & 0 & \sigma_e \end{pmatrix}. \tag{A37}$$

$$\underline{\sigma}_i = \begin{pmatrix} \sigma_i & 0 & 0 \\ 0 & \sigma_i & 0 \\ 0 & 0 & \sigma_i \end{pmatrix}. \tag{A38}$$

When $\mathbf{E} = E_x\,\mathbf{e}_x$, fluid velocities calculated with Eqs. (A17), (A24), (A26), (A27), (A37), and (A38) are as follows:

$$\mathbf{u}_e = \mathbf{u}_{ex} = -\frac{eE_x\tau_{ei}}{m_e}\mathbf{e}_x, \tag{A39}$$

$$\mathbf{u}_i = \mathbf{u}_{ix} = \frac{ZeE_x\tau_{ie}}{m_i}\mathbf{e}_x. \tag{A40}$$

As expected, in the collisional limit ($\omega_{ce}\tau_{ei}\to 0$, $\omega_{ci}\tau_{ie}\to 0$), the characteristic time between interparticle collisions is so short that, to a good approximation, electrons and ions cannot accelerate to velocities sufficiently high to be significantly affected by the magnetic field. Hence in this limit, the electron and ion fluid velocities are approximately parallel to $\mathbf{E}$.

Combining Eqs. (16), (A39), and (A40) we obtain the following:

$$\mathbf{u}_{ex} = -\frac{m_i}{Zm_e}\mathbf{u}_{ix}. \tag{A41}$$

Equation (16) guarantees that in the collisional limit, when magnetic-field effects can be neglected, kinetic momentum is conserved.

4. Electron and ion resistivity tensors and fluid equations

Multiplying both sides of Eqs. (A24) and (A25) by $\underline{\sigma}_e^{-1}$, the inverse of the electron conductivity tensor, which is the electron resistivity tensor $\underline{\eta}_e$, we obtain the following:

$$\underline{\sigma}_e^{-1}\mathbf{j}_e = \underline{\eta}_e\mathbf{j}_e = \left(\underline{\sigma}_e^{-1}\underline{\sigma}_e\right)\mathbf{E} = \mathbf{E}, \tag{A42}$$

$$\underline{\eta}_e = \begin{pmatrix} \eta_e & \dfrac{B_z}{n_e ec} & 0 \\ \dfrac{-B_z}{n_e ec} & \eta_e & 0 \\ 0 & 0 & \eta_e \end{pmatrix}, \tag{A43}$$

$$\eta_e = \frac{m_e}{n_e e^2\tau_{ei}}. \tag{A44}$$

Equations (A42)–(A44) can be rewritten as a steady-state electron-fluid equation in the absence of spatial gradients:

$$n_e e\left(\mathbf{E} + \frac{\mathbf{u}_e\times\mathbf{B}}{c}\right) = -\frac{m_e n_e \mathbf{u}_e}{\tau_{ei}}. \tag{A45}$$

Equations (A24)–(A25); Eqs. (A42)–(A43); and Eq. (A45) are mathematically equivalent.

The same arguments apply to ions, and lead directly to the ion electrical-resistivity tensor $\underline{\eta}_i$:

$$\underline{\sigma}_i^{-1}\mathbf{j}_i = \underline{\eta}_i\mathbf{j}_i = \left(\underline{\sigma}_i^{-1}\underline{\sigma}_i\right)\mathbf{E} = \mathbf{E}, \tag{A46}$$

$$\underline{\eta}_i = \begin{pmatrix} \eta_i & \dfrac{-B_z}{n_i Zec} & 0 \\ \dfrac{B_z}{n_i Zec} & \eta_i & 0 \\ 0 & 0 & \eta_i \end{pmatrix}. \tag{A47}$$

$$\eta_i = \frac{m_i}{n_i Z^2 e^2\tau_{ie}}. \tag{A48}$$

Equations (A46)–(A48) can be rewritten as a steady-state ion-fluid equation in the absence of spatial gradients:

$$-n_i Ze\left(\mathbf{E} + \frac{\mathbf{u}_i\times\mathbf{B}}{c}\right) = -\frac{m_i n_i \mathbf{u}_i}{\tau_{ie}}. \tag{A49}$$

Equations (A26), (A30); Eqs. (A46), (A47); and Eq. (A49) are mathematically equivalent.

APPENDIX B: DERIVATION OF THE ELECTRON CONDUCTIVITY TENSOR FROM THE ELECTRON BOLTZMANN EQUATION

This Appendix outlines a derivation of the electron electrical-conductivity tensor from the electron Boltzmann equation in the relaxation-time approximation. The equations below are identical in form to those of the ion Boltzmann equation; hence the results of this Appendix immediately apply to the ion electrical-conductivity tensor.

The derivation below follows closely those outlined by Refs. [52–57]. We begin with Eqs. (17)–(20) of the present article, which we repeat here for convenience:

$$\frac{\partial f_e}{\partial t} + \mathbf{v}\cdot\frac{\partial f_e}{\partial \mathbf{r}} - \frac{e}{m_e}\left(\mathbf{E} + \frac{\mathbf{v}\times\mathbf{B}}{c}\right)\cdot\frac{\partial f_e}{\partial \mathbf{v}} = \left.\frac{\partial f_e}{\partial t}\right|_{\text{collisions}}, \tag{B1}$$

$$\left.\frac{\partial f_e}{\partial t}\right|_{\text{collisions}} = -\left(\frac{f_e - f_{e0}}{\tau_{ei}}\right), \tag{B2}$$

$$f_e = f_{e0} - \tau_{ei}\left.\frac{\partial f_e}{\partial t}\right|_{\text{collisions}} = f_{e0} + f_{e1}, \tag{B3}$$

$$f_{e0} = n_e\left(\frac{m_e}{2\pi k_B T}\right)^{3/2}\exp\left(\frac{-m_e\left(v_x^2 + v_y^2 + v_z^2\right)}{2k_B T}\right). \tag{B4}$$

We assume f_e is separable into spatial and velocity factors:

$$f_e = n_e(\mathbf{r})g_e(\mathbf{v}), \tag{B5}$$

where g_e is the electron velocity distribution. We express f_e as

$$f_e = n_e g_e = n_e(g_{e0} + g_{e1}) = f_{e0} + n_e g_{e1} = f_{e0} + f_{e1}, \quad \text{(B6)}$$

$$g_{e0} = \left(\frac{m_e}{2\pi k_B T}\right)^{3/2} \exp\left(\frac{-m_e\left(v_x^2 + v_y^2 + v_z^2\right)}{2k_B T}\right), \quad \text{(B7)}$$

where g_{e0} is the equilibrium velocity distribution in the absence of electric and magnetic fields.

We assume $\partial f_e/\partial t = 0$ and $\partial f_e/\partial \mathbf{r} = 0$. We assume also that the electric field is weak, so that $|f_{e1}| \ll f_{e0}$. Combining Eqs. (B1)–(B6), and noting that

$$\frac{\partial g_{e0}}{\partial \mathbf{v}} = -\frac{m_e g_{e0}}{k_B T}\mathbf{v}, \quad \text{(B8)}$$

$$(\mathbf{v} \times \mathbf{B}) \cdot \mathbf{v} = 0, \quad \text{(B9)}$$

we obtain

$$f_{e1} = -\frac{f_{e0} e\tau_{ei}}{k_B T}(\mathbf{E} \cdot \mathbf{v}) + \frac{e\tau_{ei}}{m_e}\left(\mathbf{E} \cdot \frac{\partial f_{e1}}{\partial \mathbf{v}}\right) + \frac{e\tau_{ei}}{m_e c}(\mathbf{v} \times \mathbf{B}) \cdot \frac{\partial f_{e1}}{\partial \mathbf{v}}. \quad \text{(B10)}$$

We have assumed $|f_{e1}| \ll f_{e0}$. Thus we retain the lower-order term that includes **E** and the only term that includes **B:**

$$f_{e1} = -\frac{f_{e0} e\tau_{ei}}{k_B T}(\mathbf{E} \cdot \mathbf{v}) + \frac{e\tau_{ei}}{m_e c}(\mathbf{v} \times \mathbf{B}) \cdot \frac{\partial f_{e1}}{\partial \mathbf{v}}. \quad \text{(B11)}$$

Following Refs. [52,53,56,57], we assume f_{e1} can be expressed as

$$f_{e1} = \left(\mathbf{a}_\parallel \cdot \mathbf{v}\right) + (\mathbf{a}_\perp \cdot \mathbf{v}) + [\mathbf{b}_\perp \cdot (\mathbf{v} \times \mathbf{B})], \quad \text{(B12)}$$

where

$$\mathbf{a}_\parallel = \mathbf{a}_\parallel(\boldsymbol{r},\ \varepsilon), \quad \text{(B13)}$$

$$\mathbf{a}_\perp = \mathbf{a}_\perp(\boldsymbol{r},\ \varepsilon), \quad \text{(B14)}$$

$$\mathbf{b}_\perp = \mathbf{b}_\perp(\boldsymbol{r},\ \varepsilon), \quad \text{(B15)}$$

$$\varepsilon \equiv \frac{m_e v^2}{2}. \quad \text{(B16)}$$

The symbols || and ⊥ denote quantities parallel and perpendicular to **B**, respectively.

Combining Eqs. (B9), (B11), and (B12), defining **a** by

$$\mathbf{a} = \mathbf{a}_\parallel + \mathbf{a}_\perp \quad \text{(B17)}$$

and using the vector identities

$$\frac{\partial(\mathbf{a} \cdot \mathbf{v})}{\partial \mathbf{v}} = \mathbf{a} + \left(\mathbf{v} \cdot \frac{\partial \mathbf{a}}{\partial \varepsilon}\right) m_e \mathbf{v}, \quad \text{(B18)}$$

$$\frac{\partial[\mathbf{b}_\perp \cdot (\mathbf{v} \times \mathbf{B})]}{\partial \mathbf{v}} = (\mathbf{B} \times \mathbf{b}_\perp) + \left[(\mathbf{v} \times \mathbf{B}) \cdot \frac{\partial \mathbf{b}_\perp}{\partial \varepsilon}\right] m_e \mathbf{v}, \quad \text{(B19)}$$

$$(\mathbf{v} \times \mathbf{B}) \cdot \mathbf{a}_\parallel = 0, \quad \text{(B20)}$$

$$(\mathbf{v} \times \mathbf{B}) \cdot (\mathbf{B} \times \mathbf{b}_\perp) = -(\mathbf{b}_\perp \cdot \mathbf{v}) B_z^2, \quad \text{(B21)}$$

we obtain

$$(\mathbf{a} \cdot \mathbf{v}) + [\mathbf{b}_\perp \cdot (\mathbf{v} \times \mathbf{B})] = -\frac{f_{e0} e\tau_{ei}}{k_B T}(\mathbf{E} \cdot \mathbf{v}) + \frac{e\tau_{ei}}{m_e c}[(\mathbf{v} \times \mathbf{B}) \cdot \mathbf{a}_\perp] - \frac{e\tau_{ei}}{m_e c}(\mathbf{b}_\perp \cdot \mathbf{v}) B_z^2. \quad \text{(B22)}$$

Equation (B22) is satisfied when

$$(\mathbf{a}_\parallel \cdot \mathbf{v}) + \frac{f_{e0} e\tau_{ei}}{k_B T}(\mathbf{E}_\parallel \cdot \mathbf{v}) = 0, \quad \text{(B23)}$$

$$(\mathbf{a}_\perp \cdot \mathbf{v}) + \frac{f_{e0} e\tau_{ei}}{k_B T}(\mathbf{E}_\perp \cdot \mathbf{v}) + \frac{e\tau_{ei} B_z^2}{m_e c}(\mathbf{b}_\perp \cdot \mathbf{v}) = 0, \quad \text{(B24)}$$

$$[\mathbf{b}_\perp \cdot (\mathbf{v} \times \mathbf{B})] - \frac{e\tau_{ei}}{m_e c}[\mathbf{a}_\perp \cdot (\mathbf{v} \times \mathbf{B})] = 0. \quad \text{(B25)}$$

Equations (B23)–(B25) are valid for arbitrary values of **v** when the sum of the coefficients of **v** in each of Eqs. (B23) and (B24) equals 0, and the sum of the coefficients of $\mathbf{v} \times \mathbf{B}$ in Eq. (B25) equals 0; i.e., when

$$\mathbf{a}_\parallel = \frac{-f_{e0} e\tau_{ei}}{k_B T}\mathbf{E}_\parallel, \quad \text{(B26)}$$

$$\mathbf{a}_\perp = \frac{-f_{e0} e\tau_{ei}\xi_e}{k_B T}\mathbf{E}_\perp, \quad \text{(B27)}$$

$$\mathbf{b}_\perp = \frac{-f_{e0} e^2\tau_{ei}^2\xi_e}{m_e c k_B T}\mathbf{E}_\perp, \quad \text{(B28)}$$

where

$$\xi_e = \frac{1}{1 + \omega_{ce}^2\tau_{ei}^2}, \quad \text{(B29)}$$

$$\omega_{ce} = \frac{eB_z}{m_e c}. \quad \text{(B30)}$$

The quantity ω_{ce} is the electron-cyclotron frequency.

Combining Eqs. (B6), (B12), and (B26)–(B28) gives

$$f_e = f_{e0} - \frac{f_{e0} e\tau_{ei}}{k_B T}(\mathbf{E}_\parallel \cdot \mathbf{v}) - \frac{f_{e0} e\tau_{ei}\xi_e}{k_B T}(\mathbf{E}_\perp \cdot \mathbf{v}) - \frac{f_{e0} e^2\tau_{ei}^2\xi_e}{m_e c k_B T}[\mathbf{E}_\perp \cdot (\mathbf{v} \times \mathbf{B})]. \quad \text{(B31)}$$

We assume $\mathbf{B} = B_z\,\mathbf{e}_z$ and $\mathbf{E} = E_x\,\mathbf{e}_x + E_y\,\mathbf{e}_y + E_z\,\mathbf{e}_z$; hence Eqs. (B30)–(B31) can be expressed as follows:

$$f_e = f_{e0} - \frac{f_{e0} e\tau_{ei}}{k_B T}(E_z v_z) - \frac{f_{e0} e\tau_{ei}\xi_e}{k_B T}(E_x v_x + E_y v_y) - \frac{f_{e0} e\tau_{ei}^2\omega_{ce}\xi_e}{k_B T}(E_x v_y - E_y v_x). \quad \text{(B32)}$$

The electron current density $\mathbf{j}_e = j_{ex}\mathbf{e}_x + j_{ey}\mathbf{e}_y + j_{ez}\mathbf{e}_z$. We first consider the component j_{ex}:

$$j_{ex} = -e\int_{-\infty}^{\infty}\int_{-\infty}^{\infty}\int_{-\infty}^{\infty} f_e v_x dv_x dv_y dv_z. \quad \text{(B33)}$$

Combining Eqs. (B32)–(B33) gives the following:

$$j_{ex} = \sigma_{exx}E_x + \sigma_{exy}E_y + \sigma_{exz}E_z, \quad \text{(B34)}$$

where

$$\sigma_{exx} = \frac{e^2}{k_B T} \int_{-\infty}^{\infty} \int_{-\infty}^{\infty} \int_{-\infty}^{\infty} \tau_{ei} \xi_e f_{e0} v_x^2 dv_x dv_y dv_z, \quad \text{(B35)}$$

$$\sigma_{exy} = \frac{-e^2 \omega_{ce}}{k_B T} \int_{-\infty}^{\infty} \int_{-\infty}^{\infty} \int_{-\infty}^{\infty} \tau_{ei}^2 \xi_e f_{e0} v_x^2 dv_x dv_y dv_z, \quad \text{(B36)}$$

$$\sigma_{exz} = 0. \quad \text{(B37)}$$

In this article, we define τ_{ei} to be the electron-ion momentum-transfer collision time; i.e., the characteristic time over which *kinetic* momentum is transferred due to collisions from electrons to ions. It is well known that τ_{ei} is determined by electron-electron and electron-ion collisions [29,47,51]. Throughout the article we make the simplifying assumption that τ_{ei} can be approximated as a constant. We present below an estimate of τ_{ei} in the second Born approximation, when electron-electron collisions can be neglected [53]:

$$\tau_{ei} = \frac{m_e^2 v_e^3}{4\pi n_i Z^2 e^4 \ln \Lambda}, \quad \text{(B38)}$$

$$\ln \Lambda = \left(\ln \chi - \frac{1}{2} \right) + \left[\frac{2Ze^2}{\lambda m_e v_e^2} \left(\ln \chi - \ln 2^{4/3} \right) \right], \quad \text{(B39)}$$

$$\chi = \frac{2 m_e v_e \lambda}{\hbar}, \quad \text{(B40)}$$

$$\lambda = \lambda_D = \left[\left(\frac{4\pi n_e e^2}{k_B T} \right) + \left(\frac{4\pi n_i Z^2 e^4}{k_B T} \right) \right]^{-1/2} \text{ when } \lambda_D \geqslant a, \quad \text{(B41)}$$

$$\lambda = a = \left(\frac{4\pi n_i}{3} \right)^{-1/3} \text{ when } \lambda_D \leqslant a. \quad \text{(B42)}$$

Reference [53] includes expressions for v_e that provide estimates of τ_{ei}, and elements of the electron conductivity tensor $\underline{\sigma}_e$, for two limiting cases. The following velocity gives agreement to within a factor of ∼2 with the total electron current calculated by [53] for the two cases:

$$v_e = \left(\frac{4.8 k_B T}{m_e} \right)^{1/2}. \quad \text{(B43)}$$

Treating $\tau_{ei}\xi_e$ and $\tau_{ei}^2 \xi_e$ as constants, we approximate Eqs. (B35) and (B36) as follows:

$$\sigma_{exx} = \frac{\sigma_e}{\left(1 + \omega_{ce}^2 \tau_{ei}^2\right)}, \quad \text{(B44)}$$

$$\sigma_{exy} = \frac{-\omega_{ce} \tau_{ei} \sigma_e}{\left(1 + \omega_{ce}^2 \tau_{ei}^2\right)}, \quad \text{(B45)}$$

$$\sigma_e = \frac{n_e e^2 \tau_{ei}}{m_e}. \quad \text{(B46)}$$

To calculate j_{ey} and j_{ez}, we repeat the arguments presented above:

$$j_{ey} = \sigma_{eyx} E_x + \sigma_{eyy} E_y + \sigma_{eyz} E_z, \quad \text{(B47)}$$

$$j_{ez} = \sigma_{ezx} E_x + \sigma_{ezy} E_y + \sigma_{ezz} E_z, \quad \text{(B48)}$$

where

$$\sigma_{eyx} = -\sigma_{exy}, \quad \text{(B49)}$$

$$\sigma_{eyy} = \sigma_{exx}, \quad \text{(B50)}$$

$$\sigma_{eyz} = \sigma_{ezx} = \sigma_{ezy} = \sigma_{exz} = 0, \quad \text{(B51)}$$

$$\sigma_{ezz} = \sigma_e. \quad \text{(B52)}$$

Hence

$$\mathbf{j}_e = \underline{\sigma}_e \mathbf{E}, \quad \text{(B53)}$$

$$\underline{\sigma}_e = \begin{pmatrix} \frac{\sigma_e}{\left(1 + \omega_{ce}^2 \tau_{ei}^2\right)} & \frac{-\omega_{ce} \tau_{ei} \sigma_e}{\left(1 + \omega_{ce}^2 \tau_{ei}^2\right)} & 0 \\ \frac{\omega_{ce} \tau_{ei} \sigma_e}{\left(1 + \omega_{ce}^2 \tau_{ei}^2\right)} & \frac{\sigma_e}{\left(1 + \omega_{ce}^2 \tau_{ei}^2\right)} & 0 \\ 0 & 0 & \sigma_e \end{pmatrix}, \quad \text{(B54)}$$

where $\underline{\sigma}_e$ is the second-rank electron electrical-conductivity tensor.

[1] J. M. Creedon, Magnetic cutoff in high-current diodes, J. Appl. Phys. **48**, 1070 (1977).

[2] M. Y. Wang and M. S. Di Capua, Operating point of long magnetically insulated vacuum transmission lines, J. Appl. Phys. **51**, 5610 (1980).

[3] M. S. Di Capua, Magnetic insulation, IEEE Trans. Plasma Sci. **11**, 205 (1983).

[4] C. W. Mendel, Jr., D. B. Seidel, and S. E. Rosenthal, A simple theory of magnetic insulation from basic physical considerations, Laser Part. Beams **1**, 311 (1983).

[5] K. T. Tsang and R. C. Davidson, Macroscopic cold-fluid equilibrium properties of relativistic non-neutral electron flow in a cylindrical diode, Phys. Rev. A **33**, 4284 (1986).

[6] R. I. Lawconnell and J. Neri, Theory of magnetically insulated electron flows in coaxial pulsed power transmission lines, Phys. Fluids B **2**, 629 (1990).

[7] C. W. Mendel, Jr. and S. E. Rosenthal, Modeling magnetically insulated devices using flow impedance, Phys. Plasmas **2**, 1332 (1995).

[8] W. A. Stygar, T. C. Wagoner, H. C. Ives, P. A. Corcoran, M. E. Cuneo, J. W. Douglas, T. L. Gilliland, M. G. Mazarakis, J. J. Ramirez, J. F. Seamen, D. B. Seidel, and R. B. Spielman, Analytic model of a magnetically insulated transmission line with collisional flow electrons, Phys. Rev. ST Accel. Beams **9**, 090401 (2006).

[9] P. F. Ottinger and J. W. Schumer, Rescaling of equilibrium magnetically insulated devices using flow impedance, Phys. Plasmas **13**, 063109 (2006).

[10] P. F. Ottinger, J. W. Schumer, D. D. Hinshelwood, and R. J. Allen, Generalized model for magnetically insulated transmission line flow, IEEE Trans. Plasma Sci. **36**, 2708 (2008).

[11] W. A. Stygar, P. A. Corcoran, H. C. Ives, R. B. Spielman, J. W. Douglas, B. A. Whitney, M. A. Mostrom, T. C. Wagoner, C. S. Speas, T. L. Gilliland, G. A. Allshouse, R. E. Clark, G. L. Donovan, T. P. Hughes, D. R. Humphreys, D. M. Jaramillo, M. F. Johnson, J. W. Kellogg, R. J. Leeper, F. W. Long, *et al.*, 55-TW magnetically insulated transmission-line system: Design, simulations, and performance, Phys. Rev. ST Accel. Beams **12**, 120401 (2009).

[12] D. V. Rose, T. C. Genoni, R. E. Clark, D. R. Welch, and W. A. Stygar, Electron flow stability in magnetically insulated vacuum transmission lines, Phys. Plasmas **18**, 033108 (2011).

[13] D. V. Rose, E. A. Madrid, D. R. Welch, R. E. Clark, C. B. Mostrom, W. A. Stygar, and M. E. Cuneo, Computational analysis of current-loss mechanisms in a post-hole convolute driven by magnetically insulated transmission lines, Phys. Rev. ST Accel. Beams **18**, 030402 (2015); E. A. Madrid, D. V. Rose, D. R. Welch, R. E. Clark, C. B. Mostrom, W. A. Stygar, M. E. Cuneo, M. R. Gomez, T. P. Hughes, T. D. Pointon, and D. B. Seidel, Steady-state modeling of current loss in a post-hole convolute driven by high power magnetically insulated transmission lines, *ibid.* **16**, 120401 (2013).

[14] C. Thoma, T. C. Genoni, D. R. Welch, D. V. Rose, R. E. Clark, C. L. Miller, W. A. Stygar, and M. L. Kiefer, Numerical simulation of cathode plasma dynamics in magnetically insulated vacuum transmission lines, Phys. Plasmas **22**, 032101 (2015).

[15] R. B. Spielman and D. B. Reisman, On the design of magnetically insulated transmission lines for z-pinch loads, Matter Radiat. Extremes **4**, 027402 (2019).

[16] D. R. Welch, N. Bennett, T. C. Genoni, D. V. Rose, C. Thoma, C. Miller, and W. A. Stygar, Electrode contaminant plasma effects in 10^7-A Z pinch accelerators, Phys. Rev. Accel. Beams **22**, 070401 (2019).

[17] D. V. Rose, E. M. Waisman, M. P. Desjarlais, M. E. Cuneo, B. T. Hutsel, D. R. Welch, N. Bennett, and G. R. Laity, Numerical simulations of enhanced ion current losses in the inner magnetically insulated transmission line of the Z accelerator, Phys. Rev. Accel. Beams **23**, 080401 (2020).

[18] D. R. Welch, N. Bennett, T. C. Genoni, C. Thoma, and D. V. Rose, Fast hybrid particle-in-cell technique for pulsed-power accelerators, Phys. Rev. Accel. Beams **23**, 110401 (2020).

[19] N. Bennett, D. R. Welch, G. Laity, D. V. Rose, and M. E. Cuneo, Magnetized particle transport in multi-MA accelerators, Phys. Rev. Accel. Beams **24**, 060401 (2021).

[20] K. Tummel, D. R. Welch, D. V. Rose, A. J. Link, and K. R. LeChien, Impact of power flow on Z-pinch loads, Phys. Plasmas **29**, 113102 (2022).

[21] N. Bennett, D. R. Welch, K. Cochrane, K. Leung, C. Thoma, M. E. Cuneo, and G. Frye-Mason, Electrode plasma formation and melt in Z-pinch accelerators, Phys. Rev. Accel. Beams **26**, 040401 (2023).

[22] K. Tummel, A. J. Link, D. R. Welch, D. V. Rose, W. A. Stygar, B. T. Hutsel, and K. R. LeChien, Power flow in magnetically insulated transmission lines with ion backscatter effects, Phys. Plasmas **30**, 093506 (2023).

[23] G. K. Parks, *Physics of Space Plasmas* (Addison-Wesley, Redwood City, CA, 1991).

[24] A. Piel, *Plasma Physics* (Springer, Heidelberg, 2010).

[25] R. Feynman, R. B. Leighton, and M. Sands, *The Feynman Lectures on Physics* (Addison Wesley, White Plains, NY, 2005), Secs. 43-1–43-3.

[26] P. L. Bhatnagar, E. P. Gross, and M. Krook, A model for collision processes in Gases. I. small amplitude processes in charged and neutral one-component systems, Phys. Rev. **94**, 511 (1954).

[27] N. A. Krall and A. W. Trivelpiece, *Principles of Plasma Physics* (McGraw–Hill, New York, 1973).

[28] M. N. Rosenbluth, W. M. MacDonald, and D. L. Judd, Fokker-Planck equation for an inverse-square force, Phys. Rev. **107**, 1 (1957).

[29] L. Spitzer, Jr., *Physics of Fully Ionized Gases* (John Wiley & Sons, New York, 1962).

[30] D. Montgomery, G. Joyce, and L. Turner, Fokker-Planck equation for a plasma in a magnetic field, Phys. Fluids **17**, 954 (1974).

[31] D. Montgomery, G. Joyce, and L. Turner, Magnetic field dependence of plasma relaxation times, Phys. Fluids **17**, 2201 (1974).

[32] B. Šesták, Some properties of a collision term of a kinetic equation in a magnetic field, Czech. J. Phys. **31**, 1010 (1981).

[33] A. J. Brizard, A guiding-center Fokker–Planck collision operator for nonuniform magnetic fields, Phys. Plasmas **11**, 4429 (2004).

[34] J. Decker, Y. Peysson, A. J. Brizard, and F.-X. Duthoit, Orbit-averaged guiding-center Fokker–Planck operator for numerical applications, Phys. Plasmas **17**, 112513 (2010).

[35] H. Sugama, T.-H. Watanabe, and M. Nunami, Effects of collisions on conservation laws in gyrokinetic field theory, Phys. Plasmas **22**, 082306 (2015).

[36] C. Dong, W. Zhang, and D. Li, Fokker-Planck equation in the presence of a uniform magnetic field, Phys. Plasmas **23**, 0812105 (2016).

[37] M. Bostan, High magnetic field equilibria for the Fokker–Planck–Landau equation, Ann. Inst. H. Poincaré Anal. Non Linéaire **33**, 899 (2016).

[38] C. Dong, W. Zhang, J. Cao, and D. Li, Derivation of the magnetized Balescu-Lenard-Guernsey collision term based on the Fokker-Planck approach, Phys. Plasmas **24**, 122120 (2017).

[39] S. Cohen, E. Sarid, and M. Gedalin, Fokker-Planck coefficients for a magnetized ion-electron plasma, Phys. Plasmas **25**, 012311 (2018).

[40] S. Cohen, E. Sarid, and M. Gedalin, Collisional relaxation of a strongly magnetized ion-electron plasma, Phys. Plasmas **26**, 082105 (2019).

[41] C. Dong and D. Li, Strong magnetic field effects on the collision term and electron-ion-temperature relaxation, J. Fusion Energy **39**, 390 (2020).

[42] W. W. Heidbrink and R. B. White, Mechanisms of energetic-particle transport in magnetically confined plasmas, Phys. Plasmas **27**, 020901 (2020).

[43] A. von Boetticher, F. I. Parra, and M. Barnes, Linearised Fokker–Planck collision model for gyrokinetic simulations, Plasma Phys. Control. Fusion **66**, 105016 (2024).

[44] D. Babson, S. P. Reynolds, R. Bjorkquist, and D. J. Griffiths, Hidden momentum, field momentum, and electromagnetic impulse, Am. J. Phys. **77**, 826 (2009).

[45] D. J. Griffiths, Resource Letter EM-1: Electromagnetic momentum, Am. J. Phys. **80**, 7 (2012).

[46] F. F. Chen, *Introduction to Plasma Physics and Controlled Fusion* (Springer, Switzerland, 2018).

[47] S. I. Braginskii, in *Review of Plasma Physics* (Consultants Bureau, New York, 1965), Vol. 1, p. 205.

[48] R. J. Goldston and P. H. Rutherford, *Introduction to Plasma Physics* (Institute of Physics, Bristol, 2000).
[49] J. P. Freidberg, *Plasma Physics and Fusion Energy* (Cambridge University Press, Cambridge, UK, 2007).
[50] H. J. Lee, *Fundamentals of Theoretical Plasma Physics* (World Scientific, Singapore, 2019), pp. 29–30.
[51] E. M. Epperlein and M. G. Haines, Plasma transport coefficients in a magnetic field by direct numerical solution of the Fokker–Planck equation, Phys. Fluids **29**, 1029 (1986).
[52] Y. T. Lee and R. M. More, An electron conductivity model for dense plasmas, Phys. Fluids **27**, 1273 (1984).
[53] W. A. Stygar, G. A. Gerdin, and D. L. Fehl, Analytic electrical-conductivity tensor of a nondegenerate Lorentz plasma, Phys. Rev. E **66**, 046417 (2002).
[54] H. A. Lorentz, *The Theory of Electrons* (G. E. Stechert and Co., New York, 1909), pp. 266–273.
[55] R. E. Marshak, The radiative and conductive opacities under white dwarf conditions, Ann. N. Y. Acad. Sci. **41**, 49 (1941).
[56] C. Kittel, *Elementary Statistical Physics* (John Wiley & Sons, New York, 1958), pp. 192–205.
[57] R. Kubo, *Statistical Mechanics* (North-Holland, New York, 1965), pp. 362–373 and 393–394.